Simultaneous injection of water above gas for improved sweep in Gas EOR: An analytical and simulation study on non-uniform injection and sweep

Rahul Ranjan

Delft University of Technology

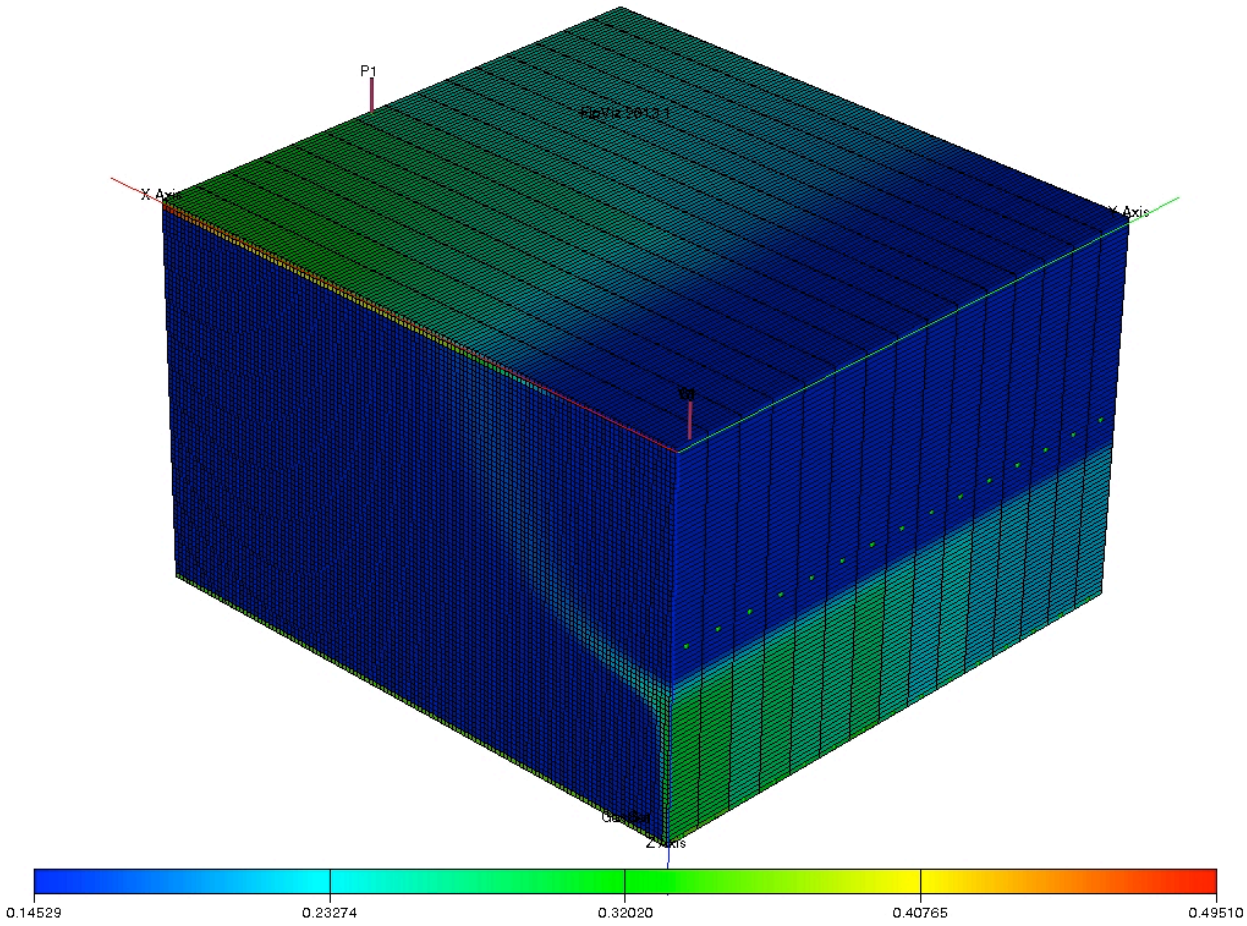

TU Delft Delft University of

Title	:	Simultaneous injection of water above gas for improved sweep in gas enhanced oil recovery (EOR): An analytical and simulation study on non-uniform injection and sweep
Author	:	Rahul Ranjan
Date	:	September 18, 2015
Professor(s)	:	Prof. Dr. W.R. Rossen

Postal Address	:	Section for Petroleum Engineering Department of Geoscience & Engineering Delft University of Technology P.O. Box 5028 The Netherlands
Telephone	:	(31) 15 2781328 (secretary)
Telefax	:	(31) 15 2781189

Acknowledgements

This project is a result of productive contribution of many people. I would like to express my sincere gratitude to each one of them for their continuous support and guidance.

I would, first, like to express my deep sense of thanks and gratitude to my thesis supervisor, Prof. Dr. William R. Rossen, for providing me an opportunity to work under his able guidance and for his continuous support and encouragement throughout the journey of this thesis and beyond. I really appreciate and would like to thank him for taking out time from his busy schedule, every week, to discuss and solve the problems together and give productive inputs.

I would like to thank Dr. Sebastien Vincent-Bonnieu and Ahmed Hussain for their continuous guidance and useful inputs despite having a busy schedule. Without their inputs and guidance, this project would have been a distant reality.

Further I would like to thank Dr. Alexey Sokolov (CGG-Vostok, Russia) and Andres Pereiro Torres (PDVSA Petrocedeño S.A., Venezuela) for their support and inputs on reservoir simulation and helping me through all the simulation problems through reservoir simulation forum on LinkedIn. Indeed technology has made the world so small.

I also want to thank all the committee members for spending their valuable time to read, evaluate and give inputs on my thesis.

I would also like to thank all the professors and teaching staffs who taught me and guided me over the last two years of MSc program. The success of this project solely lies on those shared knowledge. I thank TU Delft and CEG faculty for providing me a platform through their MSc program to further dilate my knowledge in petroleum engineering and geosciences.

Last but not least, I would like to dedicate this project to my family who believed in me, supported me and gave me the wings to fly. The success of mine is a result of their sacrifice, love and support. I, further, extend my heartfelt thanks to my friends for all their support and wonderful two years.

Abstract

Gas EOR processes can have microscopic displacement efficiency as large as 100%, but suffer from poor sweep of the reservoir. Injected gas has tendency to segregate at the top of the reservoir due to density difference and gravity. Water-alternating-gas injection was proposed by Caudle and Dyes (1958) to reduce the effect of adverse mobility ratio. Stone (2004) proposed a new injection scheme (sometimes called "modified SWAG") in which water and gas are injected simultaneously from parallel horizontal wells, with gas being injected from the bottom of the reservoir and water is injected from top from a site directly above the gas well. The water injected from the top impedes the vertical flow of gas, allowing it to move horizontally before the gas segregation happens. This gives a deeper penetration of gas before gravity segregation than simultaneous co-injection water and gas from the same well ("SWAG"). A recent study by Jamshidnezhad et al. (2010) examined the performance of the "modified SWAG" process in 3D and an MSc thesis (Mahalle, 2013) followed up on this work.

The first study found that the gas injection was non-uniform in nature, even in homogeneous reservoirs. The more-recent MSc thesis (Mahalle, 2013) appears to show that the non-uniform injection behavior may have been a result of poor grid refinement near the injection well. It was suggested to further investigate the effect of grid-block size on non-uniform nature of gas injection. The MSc thesis also shows that if the instability develops, it depends on complex interactions among the grid blocks along the well: the injection rate of one segment of the well depends on that in its neighbors, and the instability grows along the well from one end to the other.

This project extends the earlier studies, first, by examining the effects of grid refinement near the well. We conclude that grid refinement around the injection well doesn't seem to stop non-uniform injection and the non-uniformity of gas injection is not a simulation artifact of using grid blocks that are too large. Increasing gas-injection rate correlates with increasing non-uniformity of gas injection. Decreasing gas saturation exponent (n_g) in Corey's 2-phase model and decreasing gas viscosity (μ_g) leads to more-uniform injection. When there is no connection between neighboring grid blocks along the gas injection well, the gas injection behavior is more uniform. We further examine the effect of gas flow on hydrostatic pressure and conclude that hydrostatic pressure is involved in the non-uniform behavior of gas injection.

The results from this study indicate that the non-uniformity in gas injection is a result of coupling of various factors, such as, gas saturation, gas relative permeability, gas injectivity, effect of gas flow on hydrostatic pressure, and effect of adjacent grid blocks. When coupled together they form the self-reinforcing cycle leading to non-uniform behavior of gas injection, with most of the gas being issued from one end of the well. Segmenting the well into multiple segments helps ensure that gas issues from most of the perforations along the gas-injection wells and thus ensures better sweep.

Table of Contents

List of figures

1

Introduction

1.1 Literature review and Background studies

BP's Statistical Review of World Energy 2013 revealed that the global average recovery factor for a conventional oilfield is approximately 35%. This results in a large amount of oil left behind in the reservoir despite an existing production facility and infrastructure. As the demand for energy grows and fields of easy oil cease to produce, the oil and gas industries are turning to enhanced oil recovery (EOR) methods to improve the recovery factor and accelerate the associated production. There are several enhanced oil recovery methods, each with a difference, catering to the specific reservoir challenges and other parameters. The total efficiency of any recovery method is function of macroscopic (sweep) as well as microscopic displacement efficiency.

Gas EOR is one technique to improve oil recovery. The microscopic displacement efficiency of a gas EOR method can be almost 100% (S_{or} to gas sweep ~ 0). However, the success and effectiveness of this enhanced oil recovery method then depends on the sweep efficiency, i.e., the volume of the reservoir contacted by the injected fluid. Gas EOR process suffer from poor sweep of the reservoir. Density and mobility differences between the displacing fluid and displaced fluid, reservoir heterogeneity and gravity leads to poor sweep and causes viscous fingering and gravity segregation.

In a homogenous reservoir, sweep is mainly influenced by mobility and density differences between the displacing and displaced fluids, whereas in a heterogeneous reservoir, permeability difference plays the dominant role (Waggoner at al., 1992). Injected gas tends to segregate on top of the reservoir due to density difference and gravity. Gravity segregation between injected gas and water reduces gas sweep and oil recovery (Lake, 1989). In a homogenous reservoir, even if there were no density difference between the injected (gas) and displaced fluid (oil), the sweep would poor due to mobility difference. Viscous fingering occurs as a result of adverse mobility ratio. Caudle and Dyes (1958) proposed an injection scheme, water alternating gas (WAG) injection, to reduce the effect of adverse mobility ratio. In this method, slugs of water and gas are injected alternately, which alters the mobility of each. Thus, the combined mobility of the phases is less than the mobility of the gas, if injected alone, and this results in improved mobility ratio. However, miscible or immiscible WAG must be carefully designed, due to the possibility of injected water blocking the flow of oil and reducing the recovery. When water is injected alternately with gas, saturation of the water may increase to a point that it prevents the gas from contacting the oil, thus reducing the displacement efficiency of the WAG process. The performance of a WAG process is significantly affected by water-gas ratio, the number of WAG cycles, slug size, injection rate, cycle period, and system wettability (Chen et al., 2009). Stone (1982) and Jenkins (1984) propose a useful model for gravity segregation for steady-state gas-

water flow in a homogenous reservoir. They argue that although gas and water are injected alternately in the field, over sufficiently long time and distance, the process behaves like steady co-injection of gas and water. They derive equations for the segregation length for a rectangular or cylindrical homogeneous reservoir at steady state.

Simultaneous water and gas injection (SWAG) is another injection scheme that involves simultaneous injection of water and gas along an injection well. The density difference between water and gas provides a sweep mechanism in which water sweeps the hydrocarbon downwards and gas sweeps it upward. The two displacement mechanisms work simultaneously to establish a flood front, which increases the sweep efficiency, and hence, the oil recovery. However, a study of this method by Ma et al. (1995) concludes that loss of injection rate, primarily due to lower bottom-hole pressure, is observed during two-phase injection. This method was implemented on various fields and the performance has been analyzed. Quale et al. (2000), based on field study on Siri field in North Sea, concludes that some of the important controlling factors are injectivity in the formation, fracture-opening pressure, bottom-hole pressure and facility design.

Gharbi (2003) and Stone (2004) propose a new injection scheme. It is sometimes called “modified-SWAG” (Algharib et al., 2007). This method involves simultaneous injection of water and gas but from separate parallel horizontal wells. In this injection scheme, water is injected from the upper horizontal well and gas is injected from the lower horizontal well. The injected water sweeps the hydrocarbons downwards from top of the reservoir and gas from the bottom. The downward-moving water impedes the vertical flow of (upward-moving) gas, allowing it to travel further horizontally before segregation happens. This gives a deeper penetration of gas, before gravity segregation happens, than in simultaneous co-injection of water and gas from the same well (SWAG). Stone (2004) shows that injection of water above gas, either from a single vertical well or two separate parallel horizontal wells, results in a longer segregation distance (horizontal distance between the injection well and the point where gas and water segregate) than co-injection.

Rossen et al. (2006), based on a two-dimensional analysis, show that injection of water above gas results in a somewhat longer segregation length than can be realized with uniform co-injection of water and gas at the same injection rate. Rossen et al. also show that segregation distance for water-above-gas injection is proportional to the total injection rate. At fixed injection rate, the segregation distance is unaffected by the vertical positions or length of the injection intervals at which water and gas are injected, i.e., whether gas and water are co-injected uniformly along a vertical well, in just a portion of the interval, in separate interval along the well or in a point source along the well. However, the choice of injection interval does affect the injection pressure and may affect the shape of the zones: over-ride zone where only gas flows, mixed zone where water and gas flow, and under-ride zone where only water flows. Rossen et al. further suggest that the benefits of injecting water above gas are even greater when injection pressure is fixed rather than injection rate.

Van der Bol (2007) raises a concern about applying the injection scheme of Stone (2004) in three-dimensional (3D) case. In the 2D model of Stone (2004) and Rossen et al. (2006), all of the gas moves in counter-current direction through all the water, resulting in longer segregation length compared to uniform co-injection (where not all the gas is bound to flow through all the water). However, in a three-dimensional model, gas and water may bypass each other by selecting different flow paths, as injected water and gas may exit through different parts of their respective wells and never approach each other. Van der Bol (2007)

concludes that if the permeability along the well is slightly perturbed, gas injection along the well is not uniform, even at the start of injection. Bypassing develops faster when the permeability along the well is slightly perturbed than in a homogenous reservoir. The presence of perturbations accelerates the bypassing, but the magnitude of perturbations (as long as they are relatively small) does not alter the final magnitude of bypassing. Van der Bol observes that most of the gas issues from one end of the well or the other. However, no bypassing was evident, in the 3D simulation study, when the water and gas were injected from the same vertical well, in either a homogenous or perturbed reservoir. The reasons they proposed are the coarseness of the grid, relatively small lateral extent of the reservoir and/or low injection rate that prevents the bypassing.

Jamshidnezhad et al. (2010) report the effect of total injection rate, gas injection rate, hydrostatic pressure, injection-well position and well segmentation on the non-uniform nature of gas injection. They conclude that decreasing total injection rate and increasing vertical distance between gas- and water-injection wells correlates with increasing non-uniformity of gas injection. They also suggest that non-uniformity correlates weakly with gas-injection pressure, but more strongly with the difference in injection pressure of water- and gas-injection wells. They further speculate that, apart from the relation between gas saturation and relative permeability, the effect of gas flow on hydrostatic pressure, and hence on gas injection pressure, may play an important factor contributing to the instability. The study further shows that the gas issues from either end of the well irrespective of the reservoir size and location of water injection well. They also study a case where the gas injection well is segmented and gas is injected, at equal rate, in each segment. The injected gas issues from the ends of the well and/or from the junctions of the segments.

Mahalle (2013) considers a range of factors, like well model, well representation, rock and fluid properties, size of the reservoir, placement of water injector, effect of adjacent grid-blocks and local grid refinement around the gas injection well, to investigate the reasons behind non-uniform injection behavior. Mahalle suggests that the effect of adjacent grid-blocks does contribute to the non-uniformity of gas injection. The instability depends on complex interactions among the grid blocks along the well. The injection rate of one segment of the well depends on that in its neighbors, and the instability grows along the well from one end to the other. If there is no permeability between the neighboring grid-blocks (i.e., in the direction along the well), the injection comes out more uniformly. The difference between the injection pressures of the gas- and water-injection wells correlates with the gas-injection behavior and is mainly dependent on the distance between the wells. Mahalle further speculates that placing the injection wells close to each other results in relatively more uniform injection but may result in poor volumetric sweep. Using local grid refinement around the gas injection well led to a more uniform gas-injection behavior. Mahalle, however, suggests further investigation of the effect of grid-block size on non-uniform injection behavior of gas injection.

1.2 Objective

The literature so far suggests that the question of the cause of non-uniformity of gas injection in simultaneous injection of water above gas remains unanswered. However, significant research has been done so far to narrow the possibilities. The results of Van der Bol (2007), Jamshidnezhad et al. (2010) and Mahalle (2013) suggest that the instability might be a result of complex interaction between adjacent grid-blocks along the injection well, injection rate, the relationship between saturation and relative permeability, sensitivity to grid-block size (coarse gridding around the injection well) and the effect of gas flow on hydrostatic pressure, and therefore on injection pressure.

This thesis extends the earlier studies, first, by examining the effects of grid refinement around the well as per the suggestion of Mahalle (2013). After showing that instability is not a result of poor gridding and not a simulation artifact, we return to earlier works and study other factors that are thought to contribute to the instability. We also validate some of the results and extend these studies of Jamshidnezhad et al. (2010) and Mahalle (2013). We study the effect of the relationship between gas saturation and relative permeability and the effects of other fluid properties such as viscosity and total injection rate on non-uniformity of gas injection. We further speculate and examine the effect of gas flow on hydrostatic pressure and study the case of a segmented well. Finally we conclude with a discussion of the causes of non-uniform behavior of gas injection in simultaneous water above gas injection process (modified-SWAG).

2

Reservoir Model

The assumptions made by Jamshidnezhad et al. (2010) and Mahalle (2013) in their three-dimensional (3D) reservoir models are approximated here to allow comparison among the simulation results. One should keep in mind while comparing the results with Jamshidnezhad et al. (2010) and Mahalle (2013) that the simulators used by them are STARS^{TM} (Computer Modeling Group, Alberta, Canada) and MoRes (Shell) respectively. We use the ECLIPSE simulator (Schlumberger), version 2013.1.0.0, to represent the reservoir.

2.1 Model description

We simulate a three-dimensional reservoir with two horizontal injection wells on one end of the reservoir and one vertical production well on the opposite side of the reservoir.

- **Boundary Conditions**

The reservoir has closed boundaries. However, the last sheet of grid blocks, which contains the production well, represents an open boundary. The absolute permeability in the *x* and *y*-direction in the last sheet of grid blocks is given very high value (10000 mD) to represent an open boundary, while the absolute permeability in the *z*-direction in the same sheet is set to a very low value (0.01 mD) to maintain horizontal flow to the production well in this sheet.

- **Grid**

Grid is Cartesian. The height of the reservoir is 40 meters. The length (in the *x*-direction) is 64 meters and the width (in the *y*-direction) is 60 meters. The height of a grid block is 1.5 meters, except for the top five layers, for which the height of grid block is 0.5 meters. This is to allow finer resolution of the override zone and study in detail the movement of gas once the segregation occurs. The number of grid blocks in the *x* (direction of flow), *y* (along the horizontal injection well) and *z* (vertical) directions are 32, 15 and 30 respectively.

- **Wells**

Figure 1 shows the schematic of the reservoir model with wells. We are using the well architecture and location suggested by Mahalle (2013) to simulate the base case. The horizontal injector wells are located in the first sheet of grid blocks. The upper horizontal well injects water and the lower well injects gas. The water injector is placed in the center row of the vertical interval along the co-ordinate (1, *y*, 17) and the gas injector is placed in the lower-most row along the co-ordinate (1, *y*, 30). The production well is located in the last sheet of grid-blocks, i.e. to the side directly opposite to the side containing injector wells, along the co-ordinate (32, 7, *z*) and completed over the entire length.

2.2 Reservoir and fluid properties

In all the cases, the porosity of the reservoir is 0.25, horizontal permeability is 1000 mD, and vertical permeability is 210 mD, except in the grid blocks containing the water- and gas-injection wells and the last sheet of grid blocks containing the production well.

The reservoir is homogeneous, with slight perturbations in permeability (±10% of the reservoir values) along the injection wells, in order to trigger the non-uniform injection behavior. Van der Bol's (2007) study concludes that non-uniformity develops over time even if perturbations in permeability along injection wells are absent. If the perturbation in permeability is not included, the non-uniform injection develops more slowly, evidently initiated by round-off errors during computation (Van der Bol, 2007). We contend that if non-uniform injection is present in a (nearly) homogeneous reservoir, then it will definitely be present in heterogeneous reservoirs. **Figure 2** shows the cross-plot of horizontal and vertical permeability in the grid blocks along the gas injection well.

We study the steady-state gravity segregation of injected gas and water with no mobile oil present in the reservoir. Stone (1982; also see Rossen et al. 2006; Van der Bol, 2007; Jamshidnezhad, 2010 and Mahalle, 2013) assumes no mobile oil is left in the region near the well that is swept by gas and water. Immobile oil reduces mobility of gas and water and therefore, at fixed injection rate, injection pressure would be higher if residual oil is present. But the presence of immobile oil doesn't change the nature of gas-water segregation (Van der Bol, 2007). As mobile oil is not present, it is effectively a two-phase relative permeability model. For simplicity of not incorporating relative permeability of oil at residual saturation, we simulate the reservoir at an initial irreducible gas saturation of 0.15. In retrospect, the initial gas saturation should have been zero. Having initial residual gas saturation does not fundamentally alter our results. It only reduces water relative permeability somewhat in zones not entered by injected gas. The relative-permeability function, end-point values for saturation and Corey exponents are listed in **Appendix A.**

In principle the phases present in the reservoir must be incompressible to compare the results with previous work (Stone, 1982; Rossen et al. 2006; Van der Bol, 2007; Jamshidnezhad, 2010 and Mahalle, 2013). However, in ECLIPSE gas cannot be modeled as incompressible. Therefore we made the compressibility of gas very small to make it practically incompressible. Fluid properties are listed in **Appendix A.**

2.3 Operating constraints

The initial reservoir pressure is 140 bar. The injection wells are operating under rate control and the production well is at bottom-hole-pressure control. In all simulations the fraction of water being injected, out of the total injected fluid, is 0.29, as in Jamshidnezhad et al. (2010). The effect capillary forces are neglected by setting them to a value of zero. The total injection rate in the base case is 220 sm^3/d, which implies a water injection rate of 63.8 sm^3/d and gas injection rate of 156.2 sm^3/d. To ensure attainment of steady-state flow, we simulate for a period of 20 years.

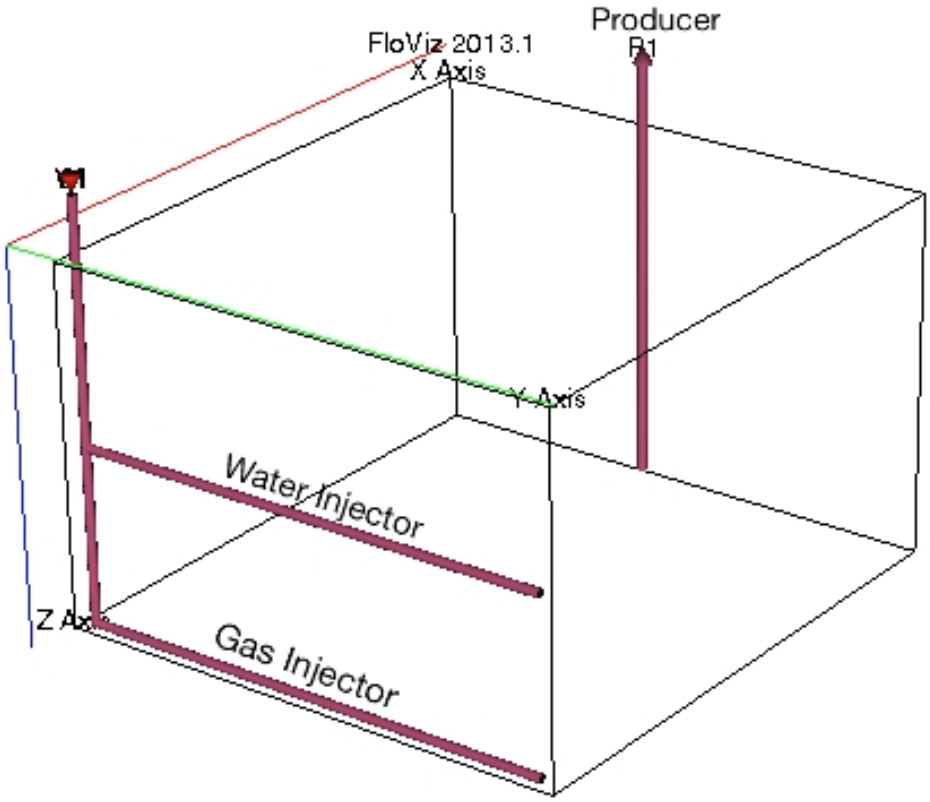

Figure 1 Schematic of three-dimensional reservoir model showing the position of wells

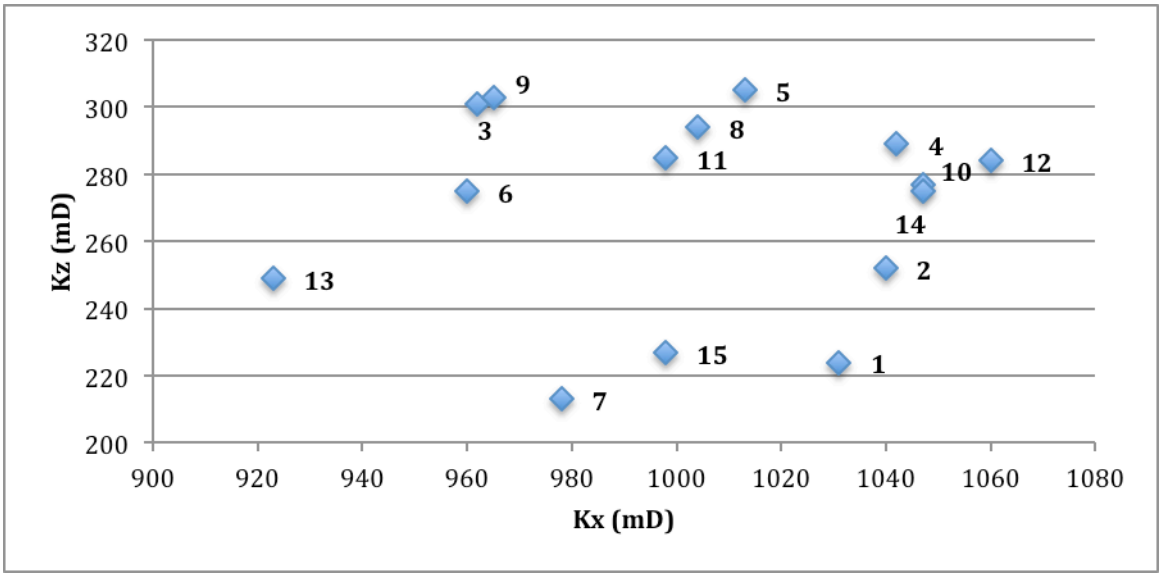

Figure 2 Cross-plot of vertical and horizontal permeability in grid blocks along the gas injection well. Numbers correspond to individual grid blocks along the gas injector, from heel to toe.

3

Results

The thesis focuses primarily on studying the non-uniform nature of gas injection along the horizontal injection well rather than estimating the segregation length. Van der Bol (2007) describes the non-uniform injection along the gas injection (horizontal) well. Jamshidnezhad et al. (2010) gives more insight on factors (injection rate, vertical distance between gas and water injector well, etc.) that affect the non-uniform nature of gas injection by simulating various cases. Mahalle (2013) considers a range of factors like well model, well representation, rock and fluid properties, size of the reservoir and near-well grid refinement. Mahalle (2013) appears to show that the non-uniform injection behavior may have been a result of poor grid refinement near the injection well and suggests further investigation of the effect of grid refinement on non-uniform gas injection. Due to lack of the dynamic model used in the study of Mahalle (2013), which was created in the simulator MoRes, we first approximately replicate the model in ECLIPSE using data provided in the study of Jamshidnezhad (2010) and Mahalle (2013). We define a base case, similar to the base-case model of Mahalle (2013), to study the non-uniform nature of gas injection. We then conduct further studies on grid refinement and various other cases. We first validate our model by comparison with the results of Jamshidnezhad et al. (2010) and Mahalle (2013).

3.1 Base Case

Our base-case total fluid injection rate is 220 m^3/day into a region of 64x60x60 m; injected water makes up 29% of total injection, while remaining fraction is gas. For the base-case model, the number of grid blocks is 32x15x30. Similar to the model of Mahalle (2013), the water injector is placed in the middle of the reservoir height, at co-ordinates (1, *y*, 17), and the gas injector is placed in the bottom-most layer, at co-ordinates (1, *y*, 30). Friction loss along the horizontal well has not been accounted in the model. The presence of frictional pressure drop may have significant effect on the behavior of the well. The pressure in the wellbore towards the heel will be higher than the pressure at the toe, so the injection pressure will vary along the perforated length. This may cause the injection rate per unit length of the well to fall off towards the toe. The lower wellbore pressure at the near end of the perforations may cause high injection in this region. To make sure that the non-uniform injection behavior is not a result of drag along the well, the frictional pressure drop is not included. The production well is operated at a bottom-hole pressure of 60 bars. Water and gas are injected at fixed rates. As the simulation reaches steady state, we see that gas injection rate is not uniform along the gas injection well (**Figure 4**), but the water injection rate is almost uniform (**Figure 5**). **Figure 3** shows gas relative permeability in each grid block along the gas-injection well at steady state. From **Figure 6** and **Figure 7**, we see that the injection starts off almost uniform, but soon after, we observe initiation of a non-uniform injection behavior. There is a continuous increasing trend in gas-injection rate near the heel and a continuous decreasing trend in injection rate as we move towards the toe of the gas injection well. Most of the gas is being issued from the heel of the gas-injection well.

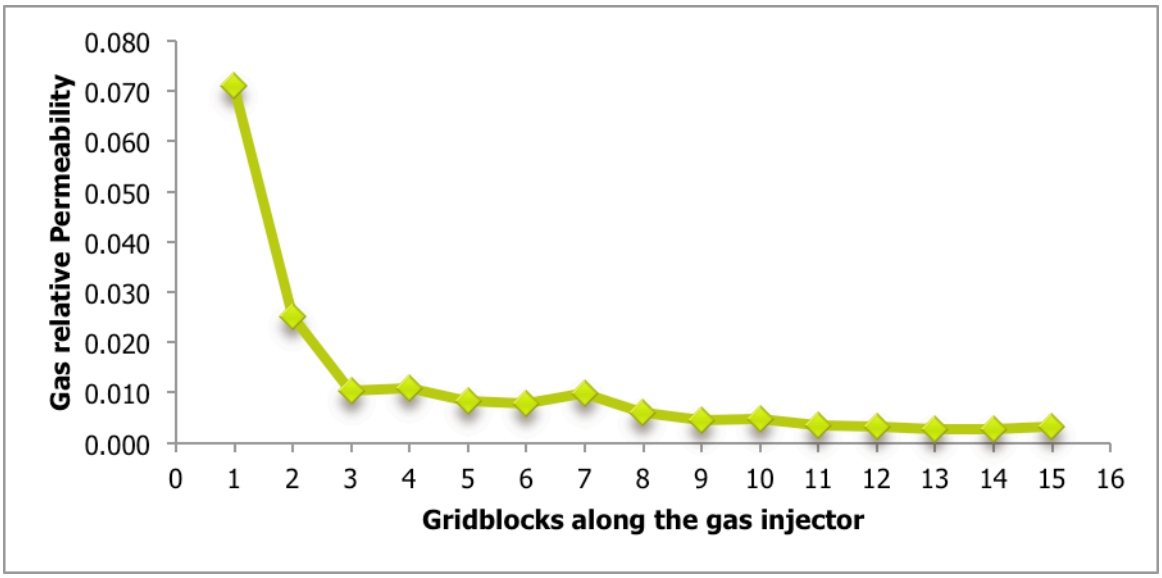

Figure 3 Relative permeability of gas in the grid blocks along the gas injection well at steady state.

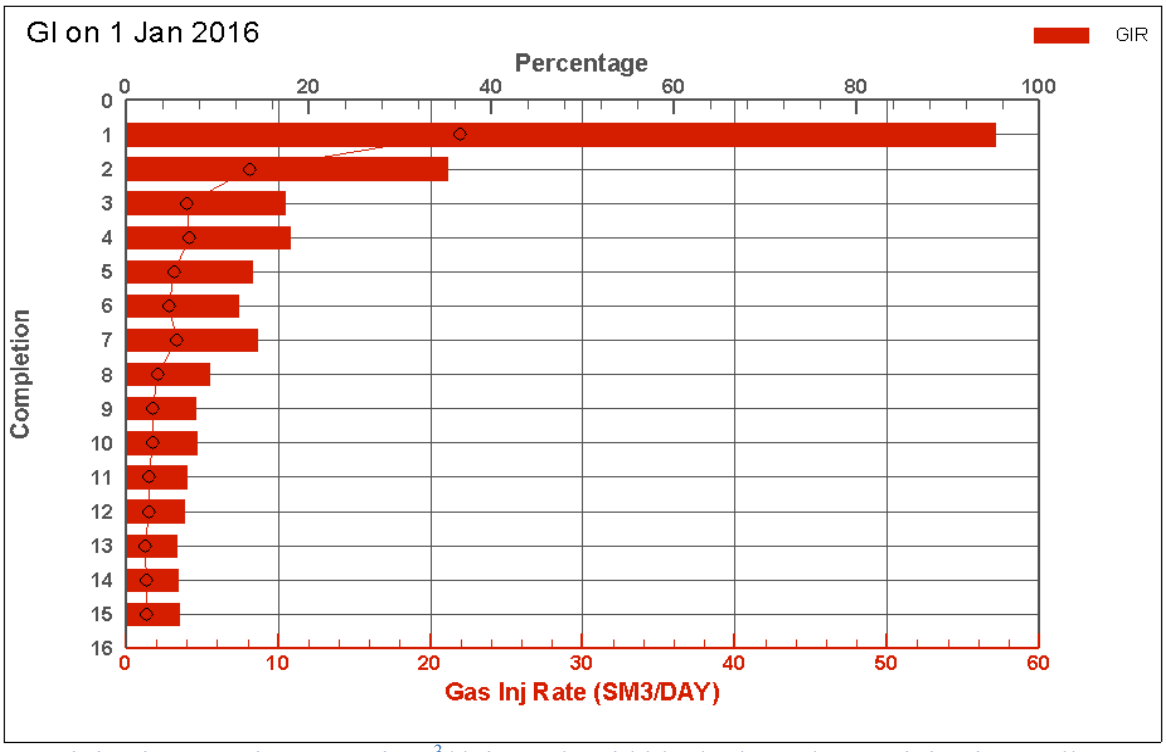

Figure 4 Gas-injection rate, in reservoir m^3/d, in each grid block along the gas-injection well at steady state after 1 year (without friction loss). Bars give gas-injection rate; circles the percent of total injection into each grid block.

Note that grid blocks 1 and 2, which together account for about half of gas injection are not the highest-permeability grid blocks along the well (**Figure 2**).

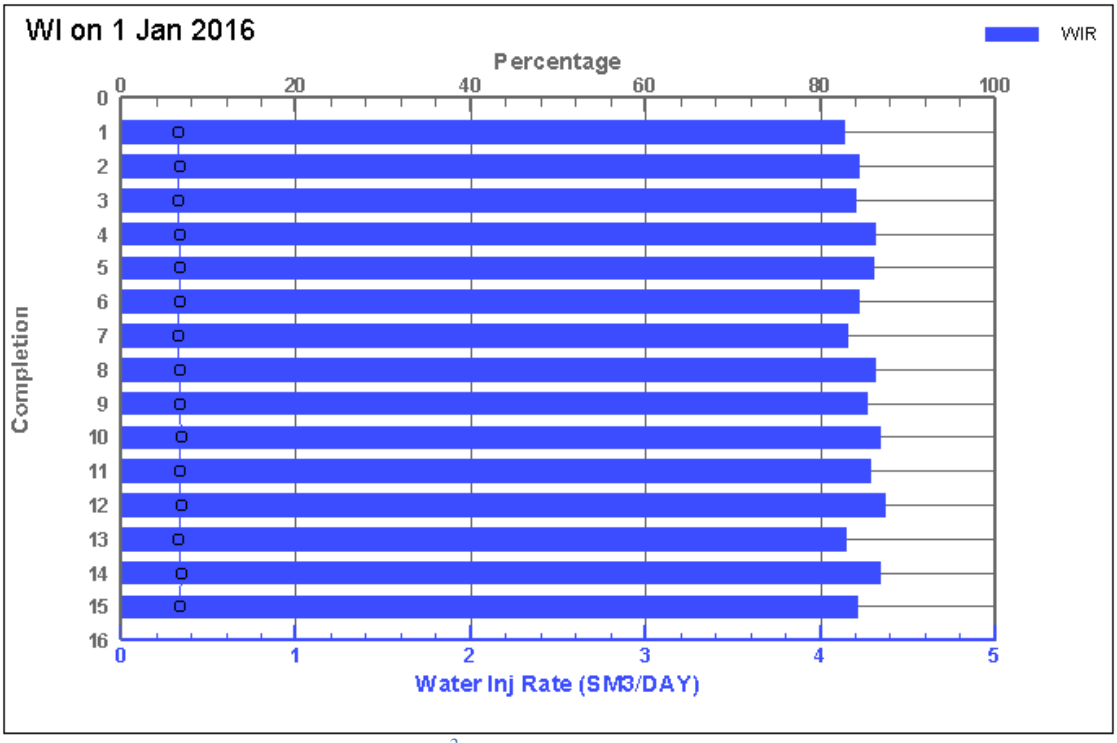

Figure 5 Water-injection rate, in reservoir m^3/d, in each grid block along the water-injection well at steady state after 1 year (without friction loss). Bars give gas-injection rate; circles the percent of total injection into each grid block.

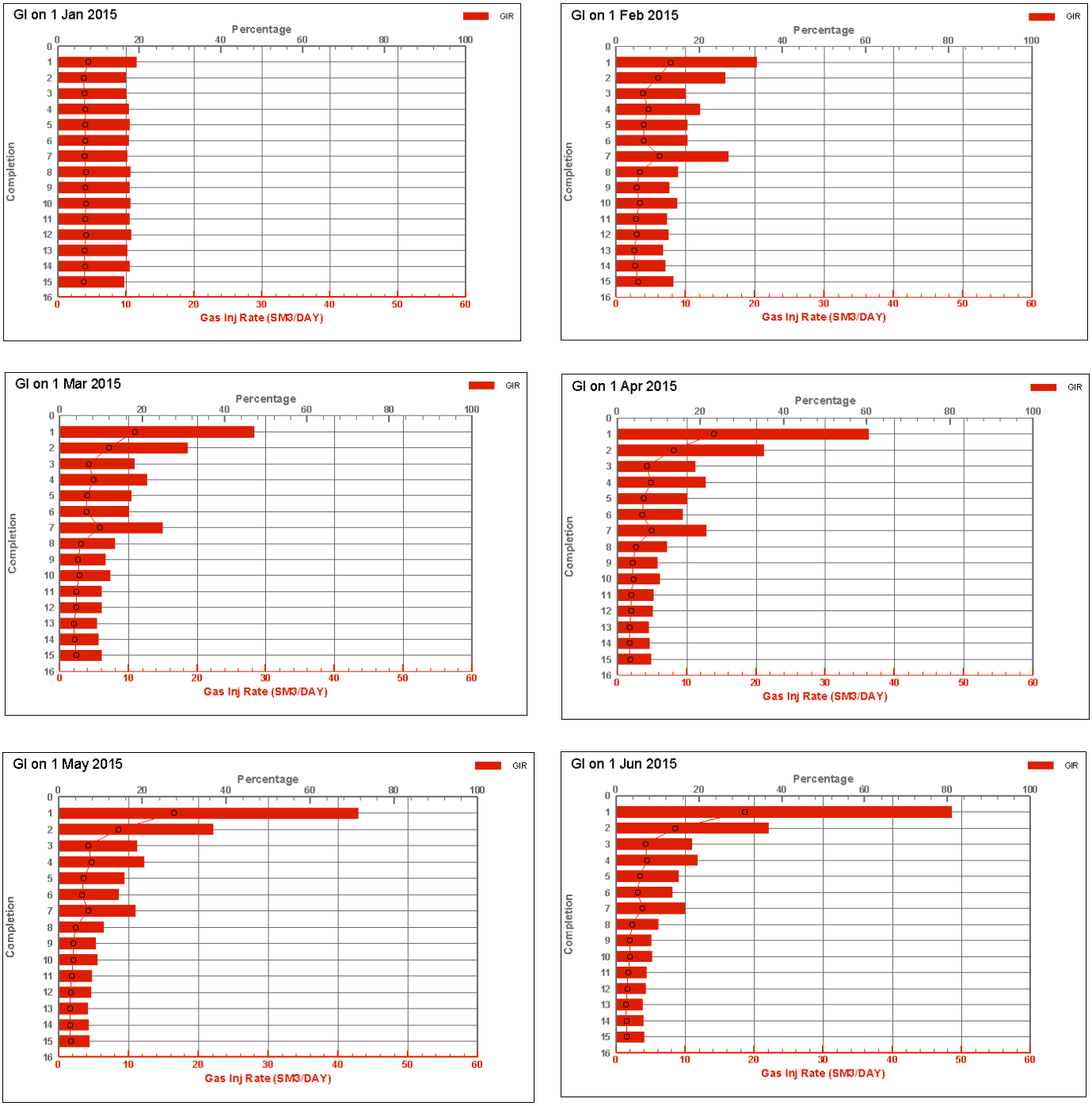

Figure 6 Gas-injection rate in each grid block along the gas injection well at different times.

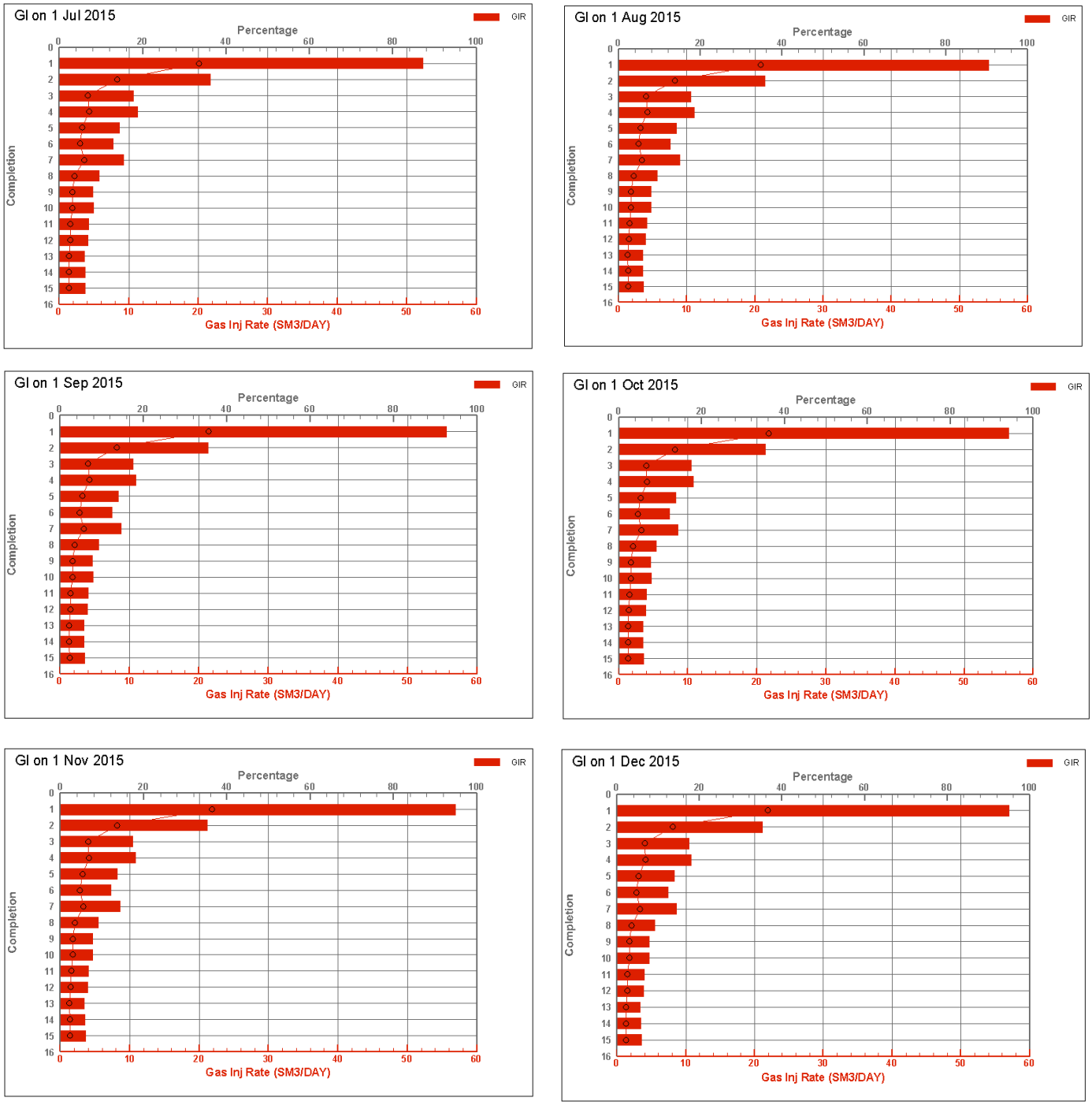

Figure 7 Gas-injection rate in the grid block along the gas injection well at different times.

3.2 Grid Refinement

Mahalle (2013) appears to show that the non-uniform injection behavior is an artifact of using too-large grid blocks along the injection well, and that local grid refinement around the injection well may solve the problem. However, this finding, and the sensitivity to the grid block size, needs to be confirmed. To study the effect of grid refinement on the non-uniform nature of gas injection, we study local grid refinement around injection well as well as a finer-grid model.

3.2.1 Local grid refinement (LGR) around injection well

We use simple grid refinement along and around the injection well. Computational time increases with more refinement. Therefore we study just two local-grid-refinement scenarios. In first scenario, which is also the scenario Mahalle (2013) used, we refine the coarse grid blocks around the injection well in the base-case model (32x15x30 grid blocks) into smaller sub-grid blocks by refining each by a factor of three in all directions (**Figure 8**). However in this case, we are dealing with too many different sizes of grid blocks, which lead to computational and linear and non-linear convergence problem. To make the transition from one size of grid block to another smooth and computationally non-problematic, we create a second scenario in which local grid refinement is created in such a fashion that we don't face such problem (**Figure 9**). In all the cases we are adopting a static local grid refinement method combined with local time stepping.

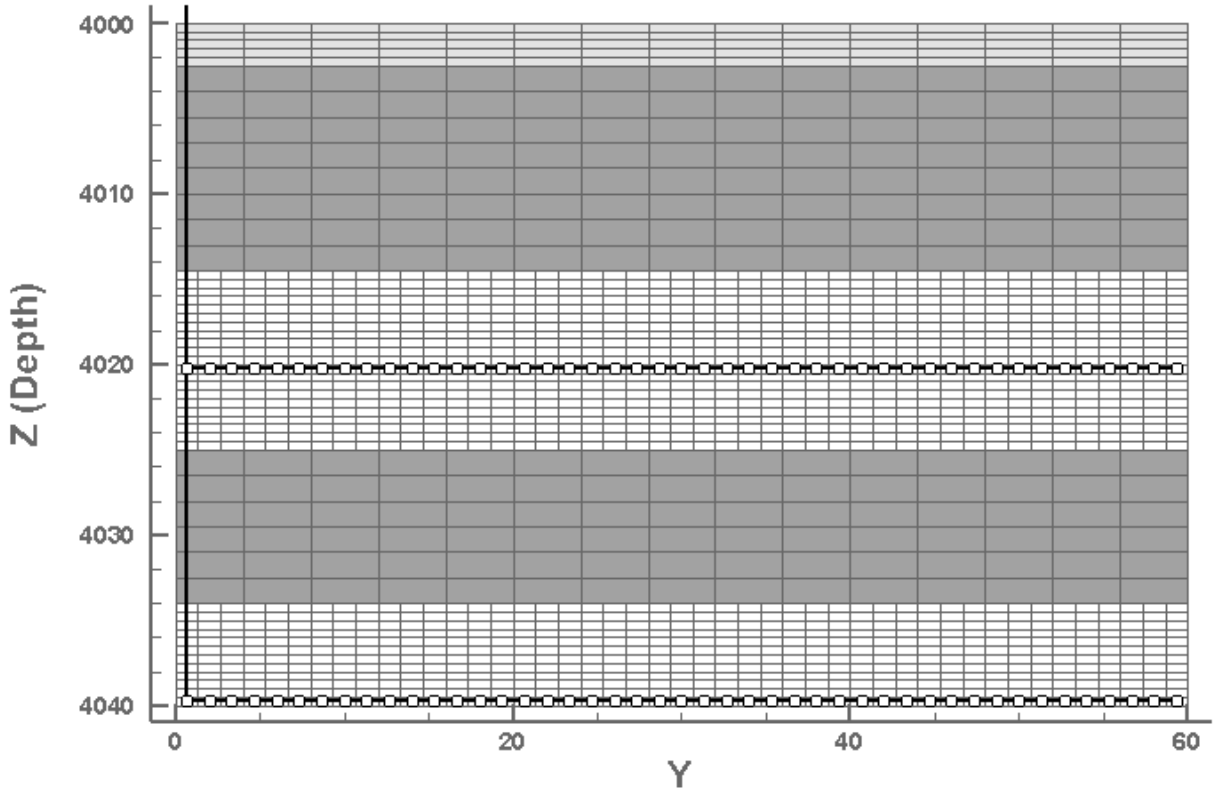

Figure 8 2D view of the local grid refinement around the injection well as per scenario 1. Grid blocks in white are refined by a factor of 3 in all directions.

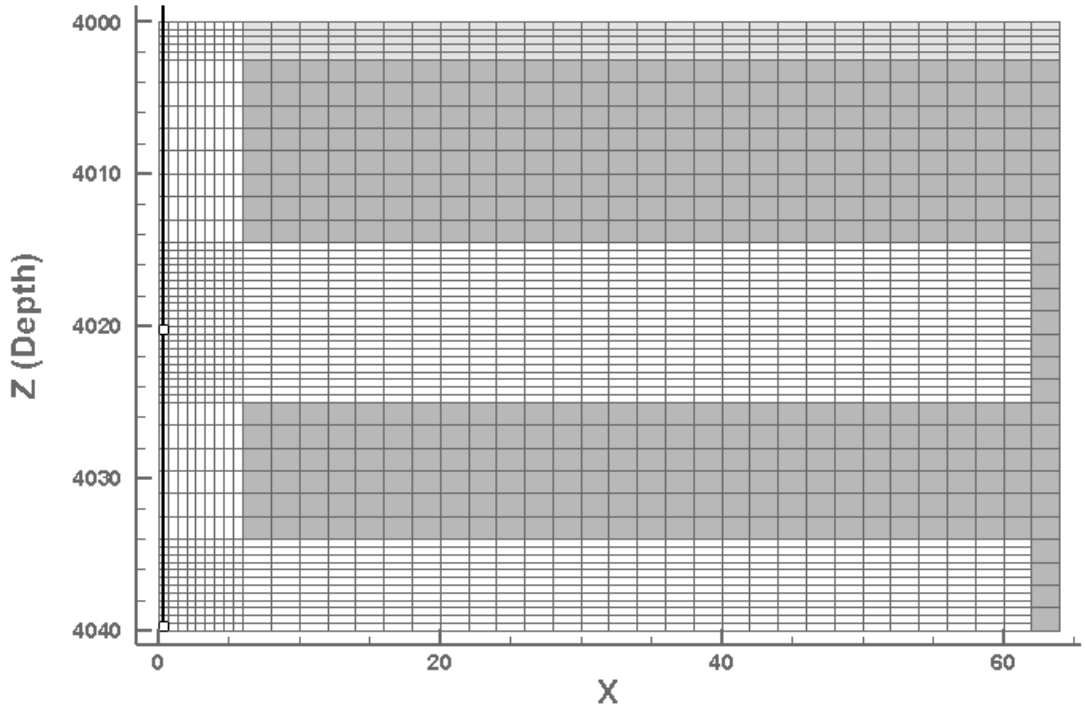

Figure 9 2D view of the local grid refinement around the injection well as per scenario 2 (side-view). Grid blocks in white are selectively refined by a factor of 3.

Figure 10 shows that the non-uniform nature of gas injection persists even after local grid refinement around the injection well as per first scenario. To further check and validate our result, we run the simulation for second scenario (scenario 2); in both the scenarios, most of the gas issues from the heel (**Figure 11**). However, as stated above, the results of first scenario (scenario 1) can't be trusted because of degree of error it involves during computation because of poor grid refining and linear & non-linear convergence problem. We are going ahead with results of second scenario, which doesn't have any such problem.

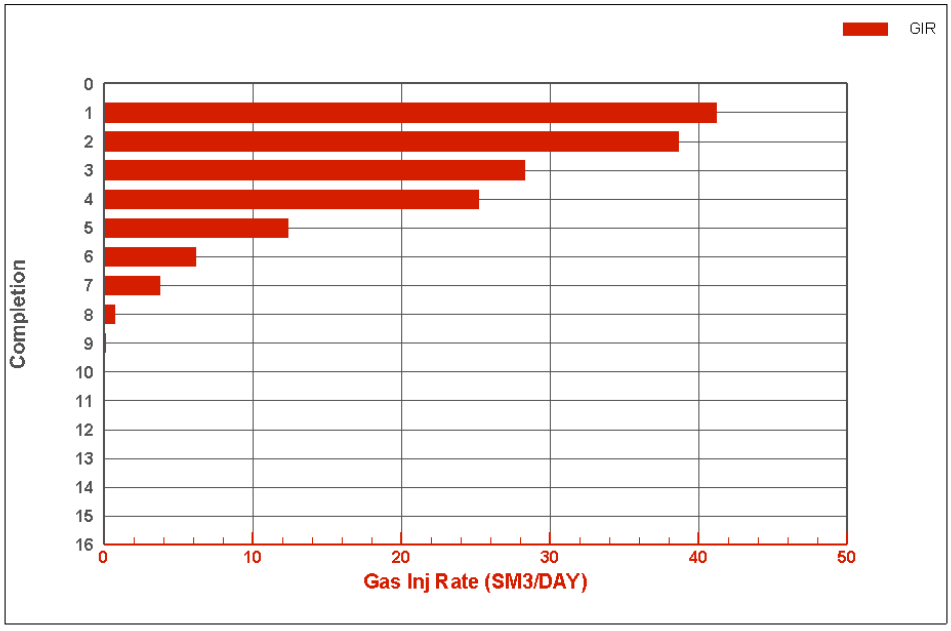

Figure 10 Gas-injection rate, in reservoir m^3/d, in each grid block along the gas-injection well at steady state after 1 year, with local grid refinement around the injection well (Scenario 1)

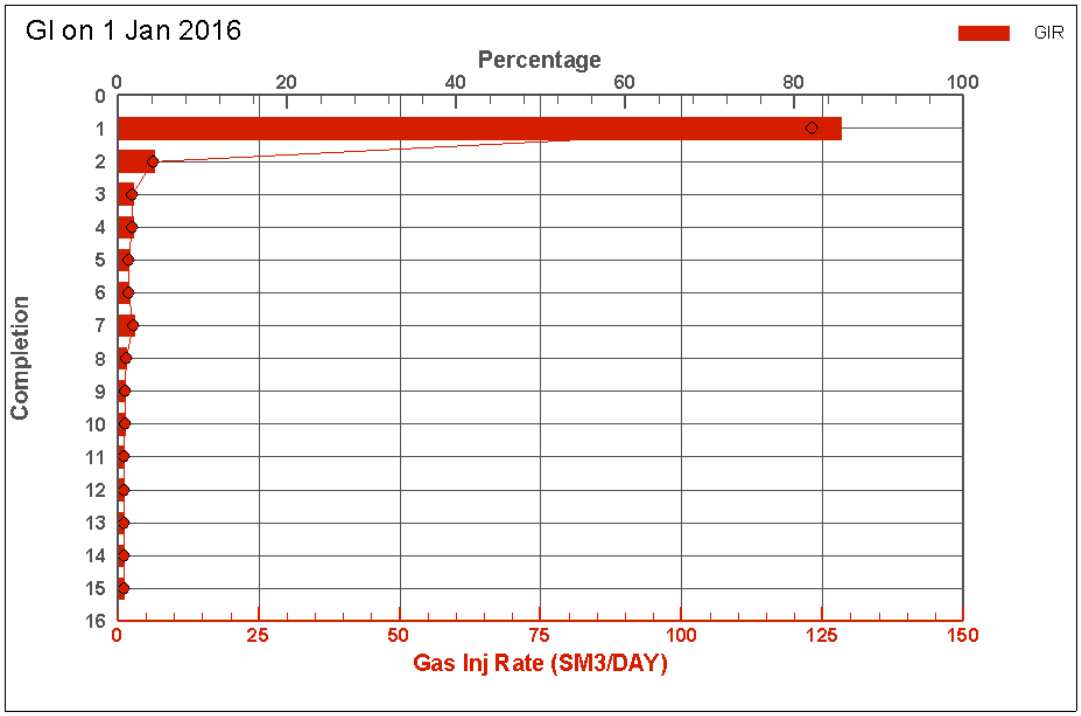

Figure 11 Gas-injection rate, in reservoir m^3/d, in each grid block along the gas-injection well at steady state after 1 year, with local grid refinement around the injection well (Scenario 2)

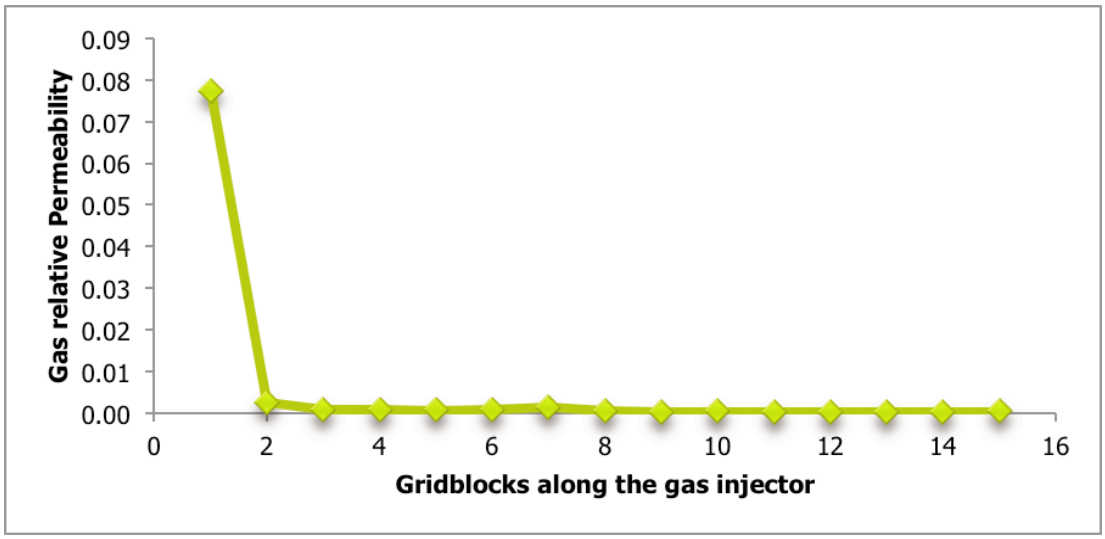

Figure 12 Relative permeability of gas in the grid blocks along the gas-injection well with local grid refinement (Scenario 2).

The results of local grid refinement around the injection well clearly show that non-uniform injection along the gas injection well is not solved by local grid refinement. Mahalle (2013), however, reports that applying local grid refinement near the injection well leads to a more-uniform gas-injection profile (**Figure 15**) and that it is possible that unstable injection was a mere an artifact of poor grid refinement near the injection well. This contradicts our results.

To further validate our result and support our argument we simulate a finer-grid model. If we observe a similar result (unstable injection) as with local grid refinement, then we can confirm that it is not a grid-refinement problem.

3.2.2 Finer-grid model

Finer-grid models are computationally time consuming, but provide a better approximation to reality than the coarse or local-grid-refinement model. This is because the error associated with the discretization method, using the finite difference method, is a function of grid-block size. If grid-block size increases by a factor of two, then the error increases by a factor of four. Similarly if the grid block size is halved, then the order of error becomes one-fourth. So using a fine-grid model increases the accuracy and decreases the degree of error. However, the computational time increases as we go to a finer-grid. To be as be fine as possible and at the same time have reasonable computation time, we decided to use a total of 128x15x80 grid blocks for the model of 64x60x40 m. We do not want to end up refining our model so fine that it's computationally extremely time consuming and requires more disk space than available. So we decided to refine the model mostly in the x- and z-directions, as the gas movement is mostly into the x- and z-directions due to gravity and density difference. A study is also shown in **Appendix D** with refinement in only the y-direction along the gas injection. But just to avoid long computation time we did not refine the grid in the *y*-direction in the fine-grid model.

Figure 13 and **Figure 14** shows that the non-uniform nature of gas injection along the horizontal injection well is still present in our fine-grid model. This further validates and substantiates our local-grid-refined model's result. The instability is not solved either by local grid refinement or finer-grid modeling. In both the cases we see that most of the gas issues from one end of the well.

Mahalle's results are not consistent regarding the effect of grid refinement. If local grid refinement (LGR) around the injection well did solve the non-uniform nature of gas injection, then his LGR results should be validated and substantiated by his finer-grid model's results, too. The result of the finer-grid model of Mahalle (2013) shows non-uniformity of gas-injection more severe than with LGR. Local grid refinement is nothing but an intermediate stage between coarse and fine grid model. Yet it's results differ from his fine-grid model. **Figure 15** shows a comparison between results generated in our case and Mahalle's (2013) case.

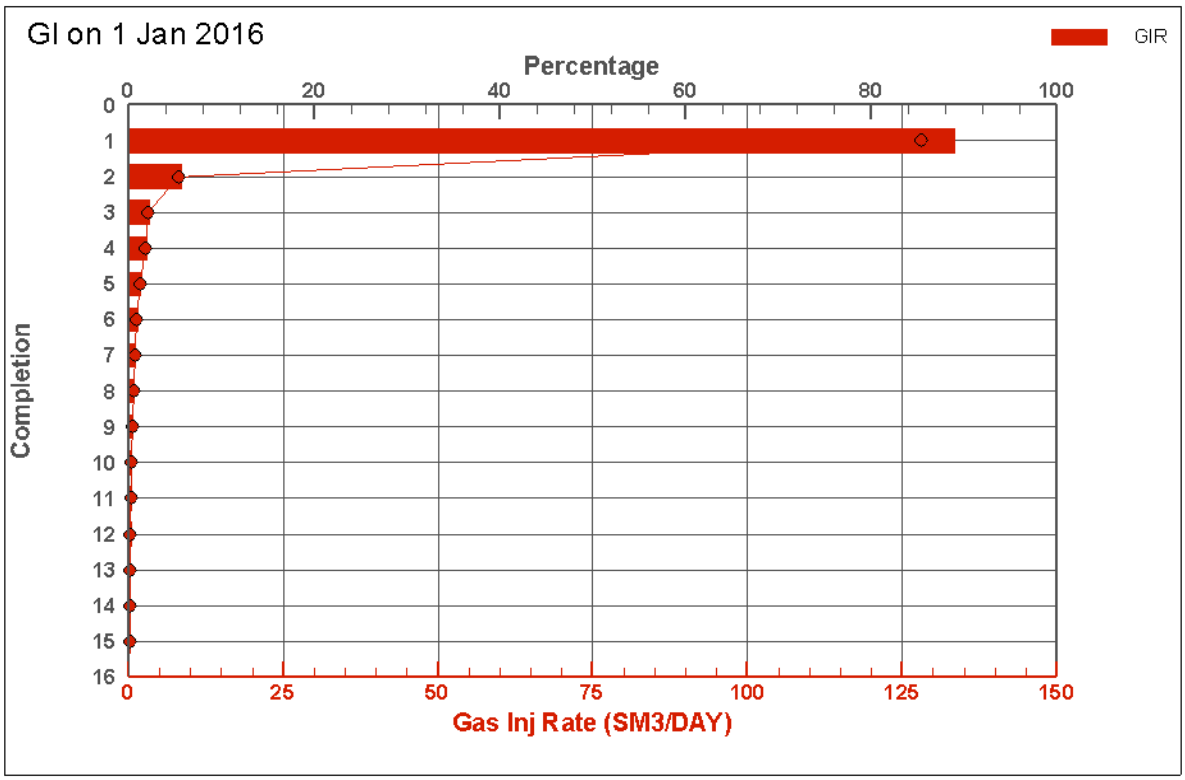

Figure 13 Gas-injection rate, in reservoir m^3/d, in each grid block along the gas-injection well at steady state after 1 year for fine-grid model

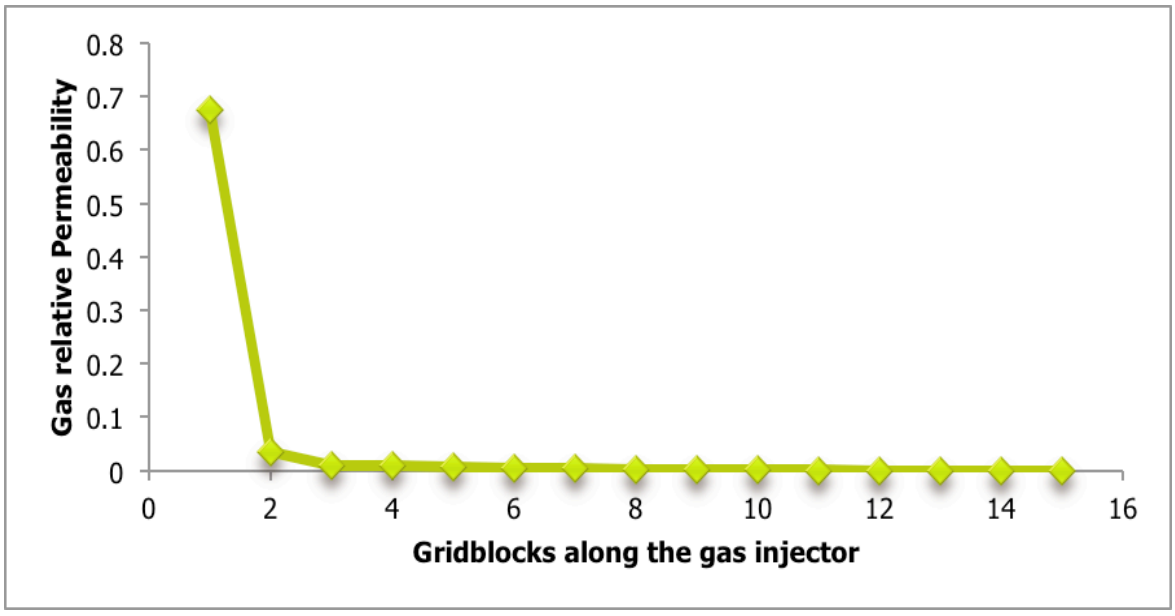

Figure 14 Relative permeability of gas in the grid blocks along the gas injection well in fine-grid model.

	Ranjan (2015)	Mahalle (2013)
Coarse (Base Case)	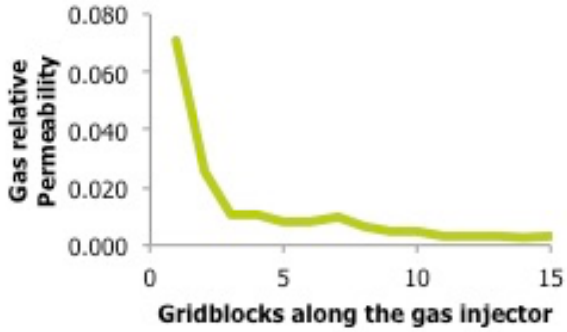	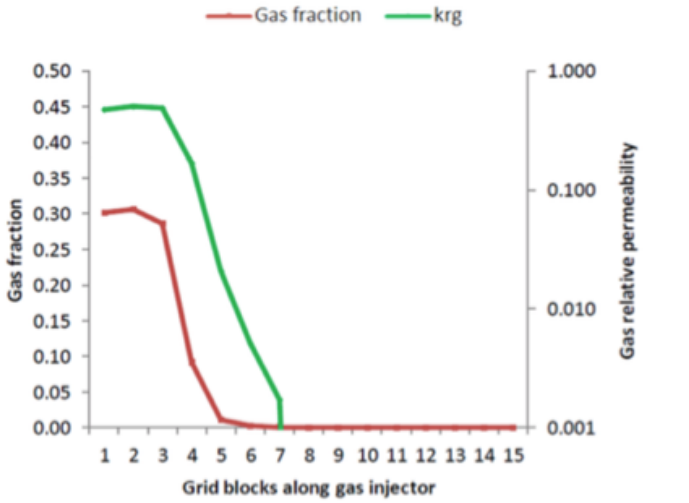
LGR	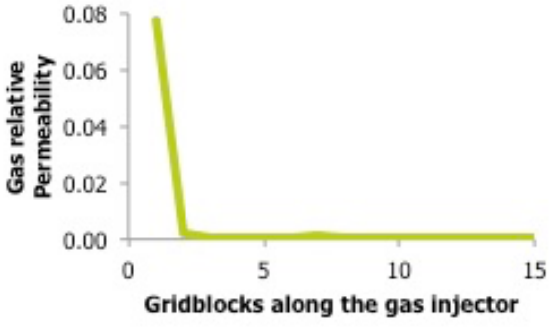	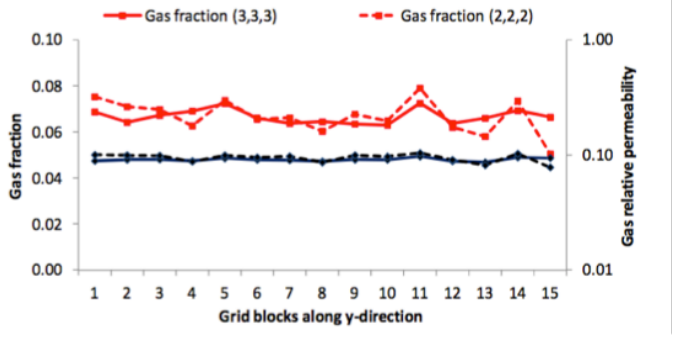
Fine	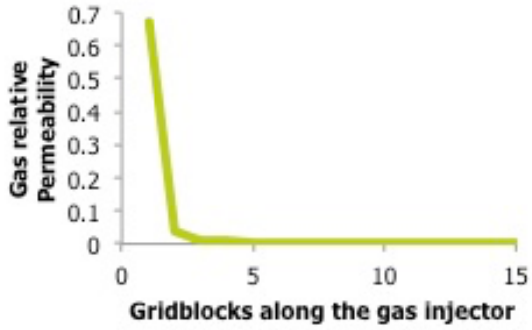	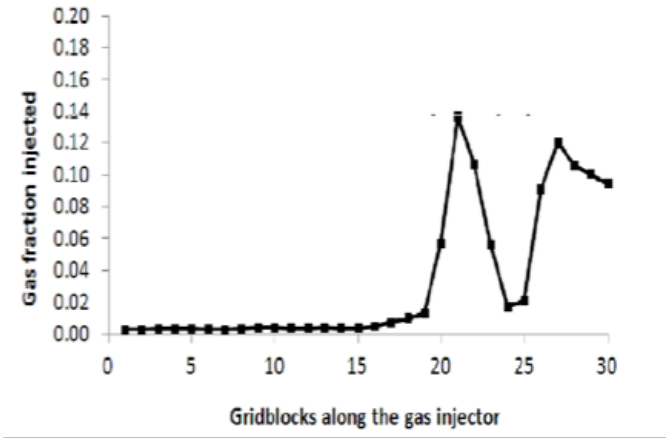

Figure 15 Comparing the results generated in our case and Mahalle's (2013) case.

In our result, we see in all the cases - Base case, LGR or Fine-grid model - the non-uniform nature of gas injection is present irrespective of grid refinement, giving a clear indication that non-uniform injection behavior is not an artifact of using grid blocks for the injection-well segments that are too large, and local grid refinement around injection well does not solve the problem.

3.3 Effect of Variation in Corey Exponent

The result with grid refinement suggests that the non-uniform injection behavior is not a result of poor gridding. We believe that the non-uniform injection behavior might be somehow associated with gas saturation and gas relative permeability. Hence we study the effect of relative-permeability model. The relative-permeability model used to simulate the base case is Corey's two-phase model. The relative-permeability function, end-point values for saturation and Corey exponents are listed in **Appendix A**. The Corey saturation exponents, used to simulate the base case, for gas and water are 2 and 2.5, respectively. They are relatively neutral and hence don't give any preferential mobility to any specific phase. We study two cases with the motive to vary the relative-permeability model and study the injection behavior. In first case, we increase the value of gas-saturation exponent to 4.2 and, in second case, we decrease the value to unity. The second case leads to a linear relationship between saturation and relative permeability.

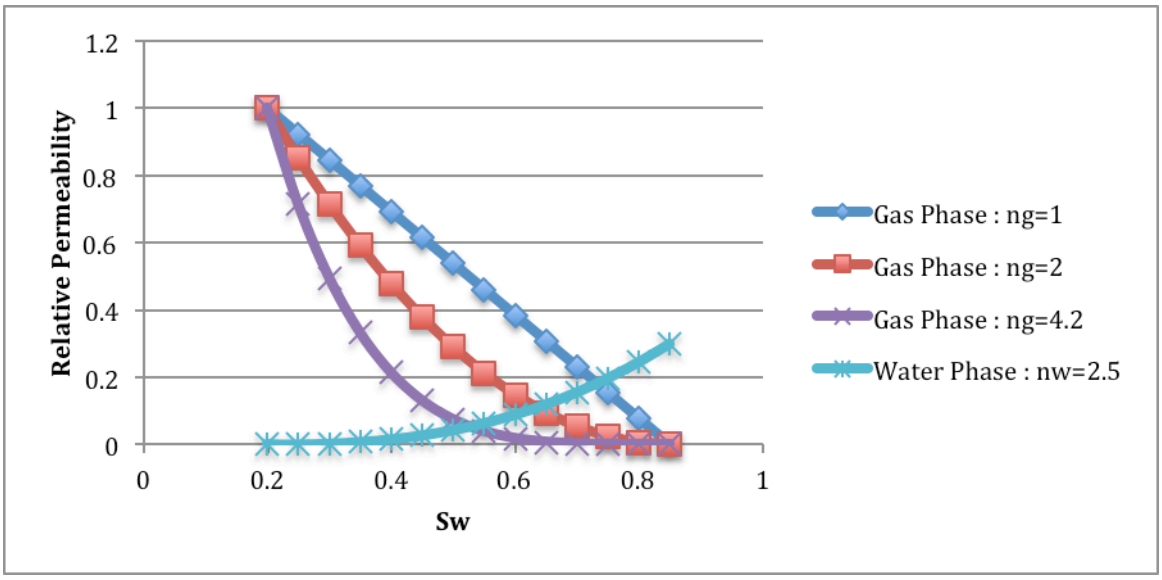

Figure 16 Plot of relative permeability of gas for various values of gas saturation exponent (n_g)

If we observe the relative-permeability curve of gas at various n_g values (**Figure 16**), we notice that for a fixed value of saturation, a decrease in the value of gas saturation exponent (n_g) increases the gas relative permeability, which subsequently increases the mobility of the gas. **Figure 17** shows that as the value of the gas saturation exponent (n_g) decreases, the gas injection tends to become more uniform.

An analysis was done to study how and by what percentage an increase in relative permeability affects the injection rate or vice versa. The analysis (**Appendix B**) shows that even a small increase in gas-injection rate leads to a significant increase in the relative permeability of gas. One of the speculations of Jamshidnezhad et al. (2010) on non-uniform injection behavior of gas injection is that higher gas injection rate gives higher gas saturation near the well, which in turn increases gas relative permeability and reinforces the increased injection rate. Our study shows that the relative increase in gas relative-permeability is less than the relative permutation in gas injection rate. In other words, a permutation would remain bounded unless reinforced by some other mechanism. Even though an increase in gas injection rate increases the gas relative permeability significantly, it is not the sole cause of the non-uniform injection behavior.

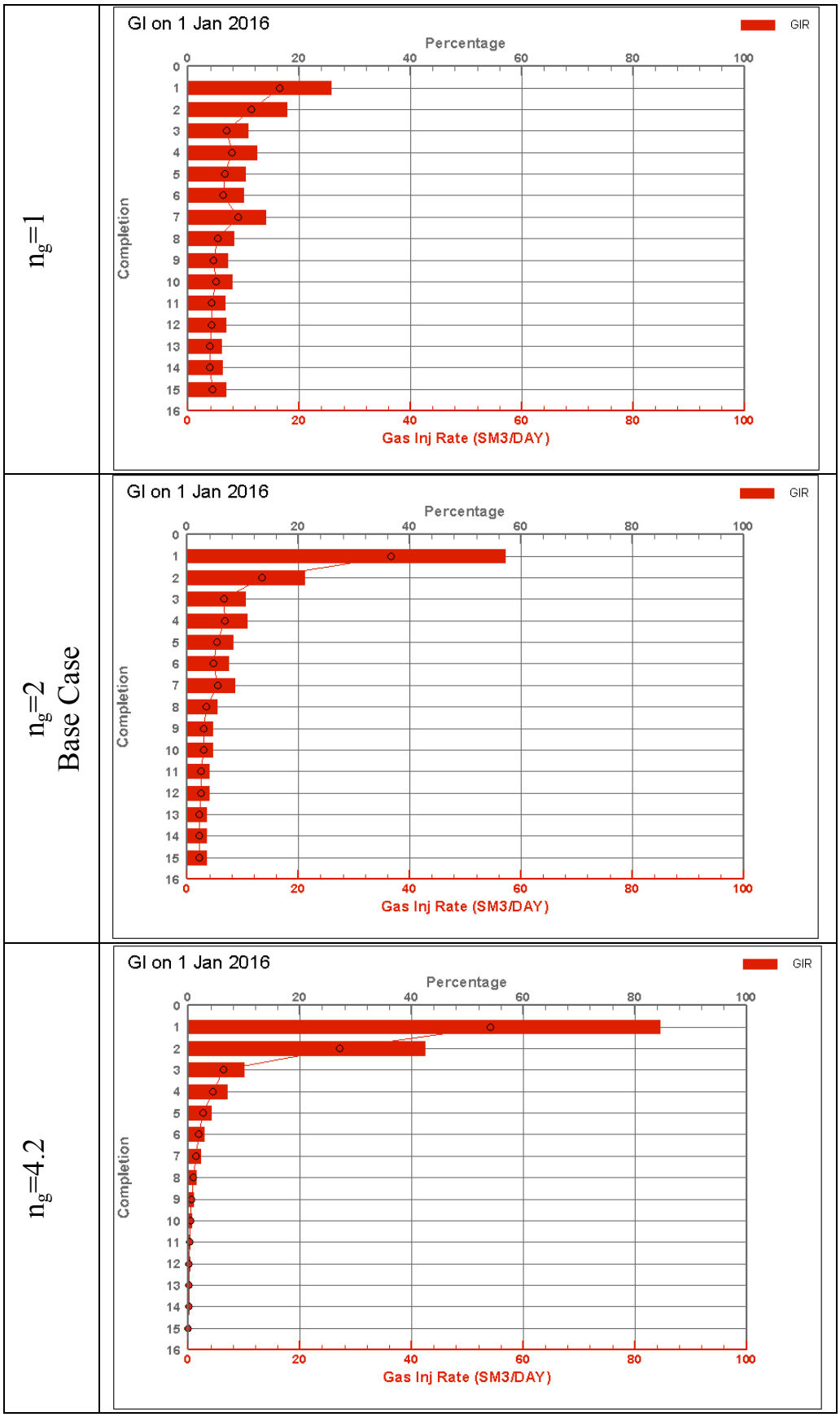

Figure 17 Gas-injection rate in each grid block along the gas-injection well for various values of the gas saturation exponent (n_g)

3.4 Varying Gas Viscosity

We vary the gas viscosity with the motive to vary the mobility of gas and cross-verify the results generated in the previous case (**Section 3.3**). **Figure 18** shows that on reducing the viscosity of gas, injection becomes more uniform and on increasing the viscosity of gas, injection becomes more non-uniform. Viscosity is inversely related to mobility. In both the cases, section 3.3 and 3.4, we observe that on increasing the mobility of the gas, the injection becomes more uniform.

3.5 Varying Gas Injection Rate

Figure 19 shows the gas injection rate in the grid blocks along the perforated length of the gas injection well for various cases, keeping all other parameters the same as that of the base case, but varying total gas-injection rate. The results show that an increase in total gas-injection rate makes the gas injection more non-uniform and a decrease in injection rate makes the gas injection behavior relatively more uniform than the base case.

The results, in our case, contradict with the results of Jamshidnezhad et al. (2010), who conclude that increasing non-uniformity of gas injection correlates with decreasing total injection rate: i.e., with injection rate halved, injection is somewhat less uniform; with injection rate doubled, somewhat more uniform. In our results, we see diametrically opposite behavior: i.e., with injection rate halved, injection becomes more uniform and with injection rate doubled, injection becomes more non-uniform.

Appendix B describes the effect of total injection rate on non-uniformity of gas injection. A higher injection rate will significantly increase the relative permeability and accelerate the instability faster than a lower injection rate. This may explain the reason behind more-uniform injection at lower injection rate.

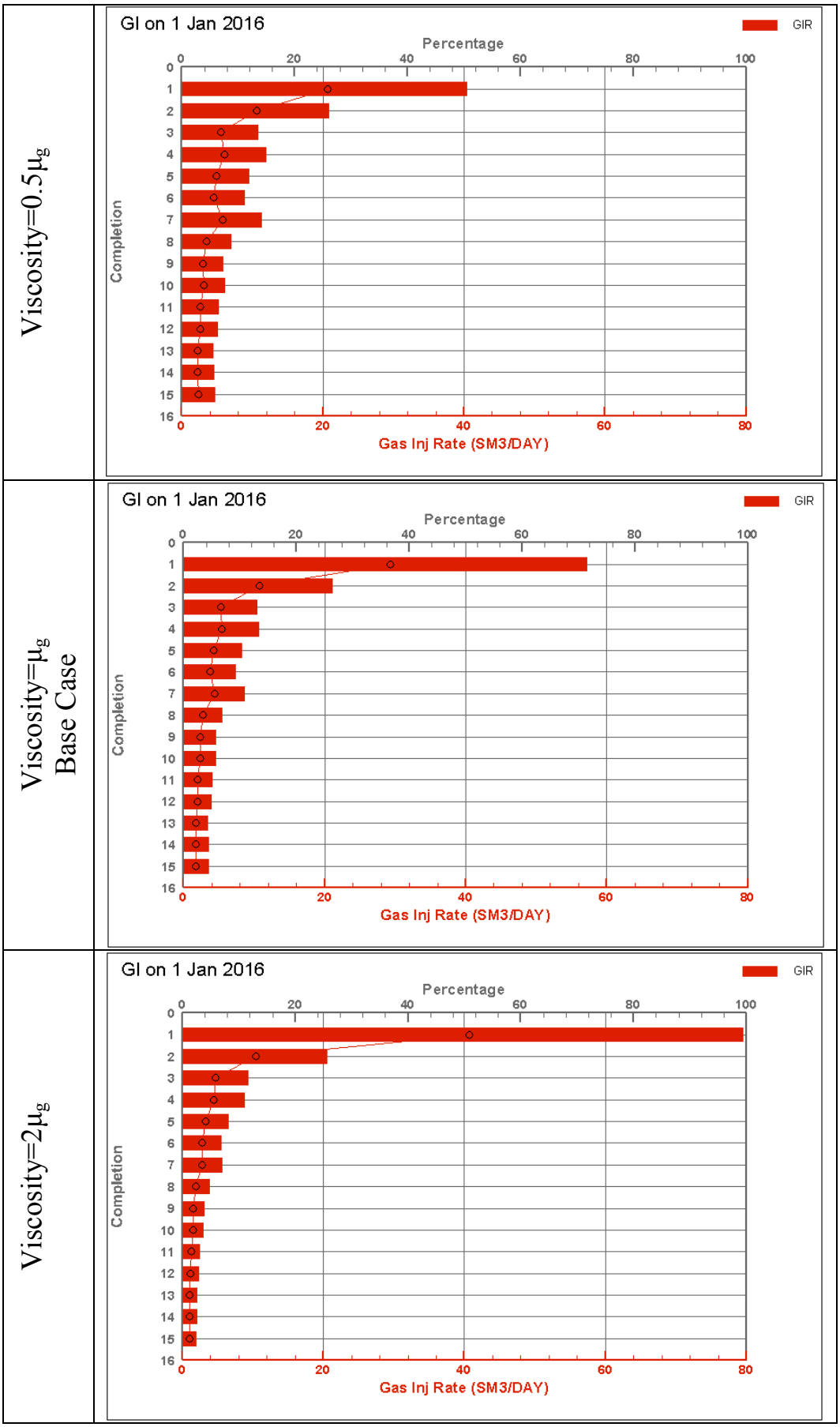

Figure 18 Gas-injection rate in each grid block along the gas-injection well for various values of gas viscosity (μ_g)

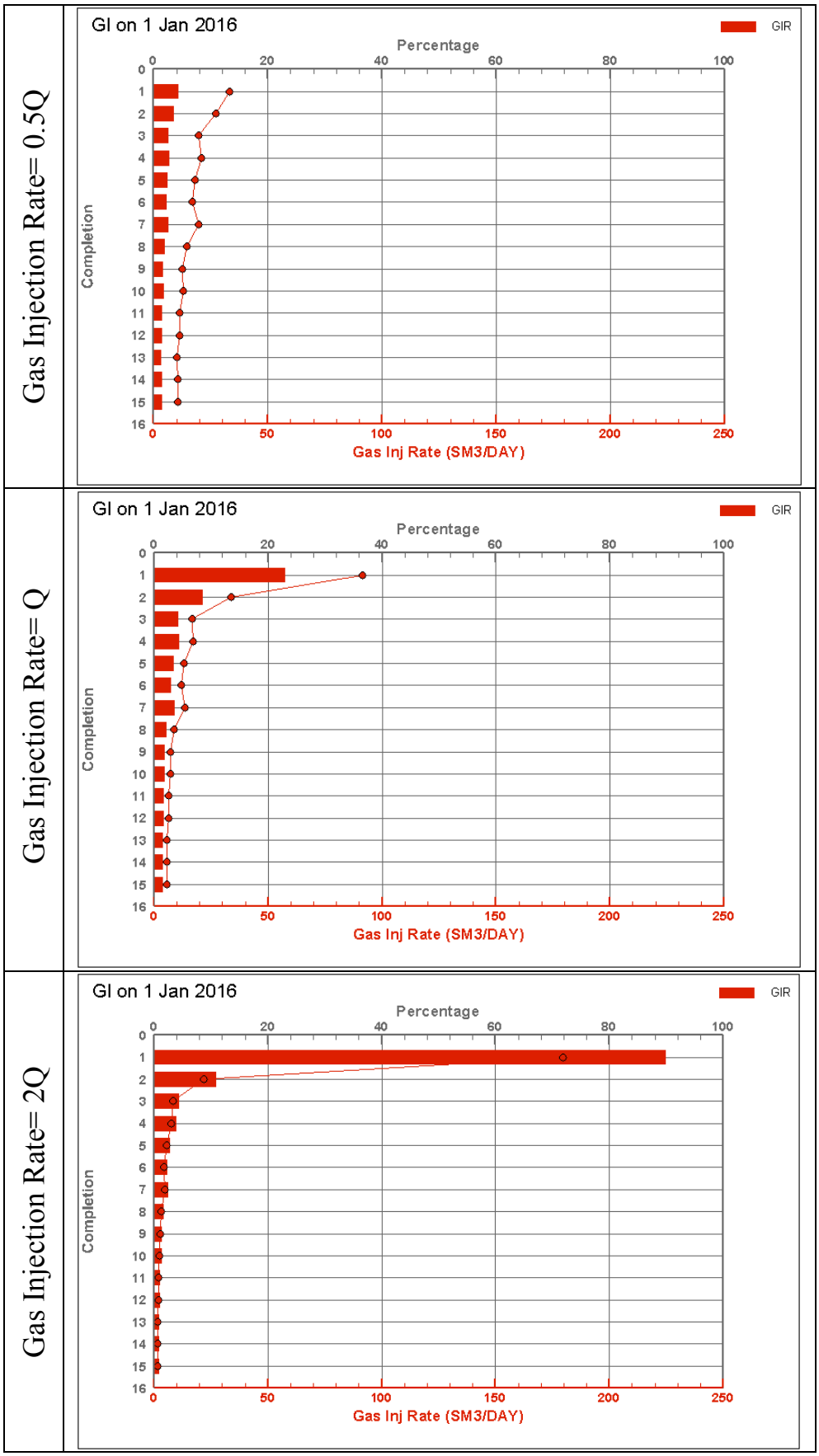

Figure 19 Gas-injection rate in the grid blocks along the perforated length of gas-injection well for different values of total gas-injection rate. Water-injection rate is kept same as in the base case.

3.6 Effect of Adjacent Grid Blocks

Mahalle (2013) suggests that the loss of uniformity in gas injection is due, at least in part, to the influence of adjacent grid blocks. To examine this suggestion, we create a model where the sheets of grid blocks perpendicular to the injection wells, extending in both *x*- and *z*-direction, are isolated from each other. The absolute permeability in the *y*-direction is reduced to a value of zero to create flow resistance in the *y*-direction and isolate the sheet of grid blocks perpendicular to the injection wells from each other. However, the last sheet of grid blocks (extending in the y-direction) that contains the production well has a high permeability value (10 Darcy) in *x*- and *y*-direction to allow easy flow to the production well. All other parameters are same as in the base case.

Figure 20 shows the gas injection rate in the grid blocks along the perforated length of the gas injection well for the above-mentioned case. We see that injection is fairly uniform when sheets of grid blocks perpendicular to each other are isolated from each other. This suggests and supports the speculations of Mahalle (2013) that non-uniform gas injection may be due, or in parts, to the influence of adjacent grid blocks.

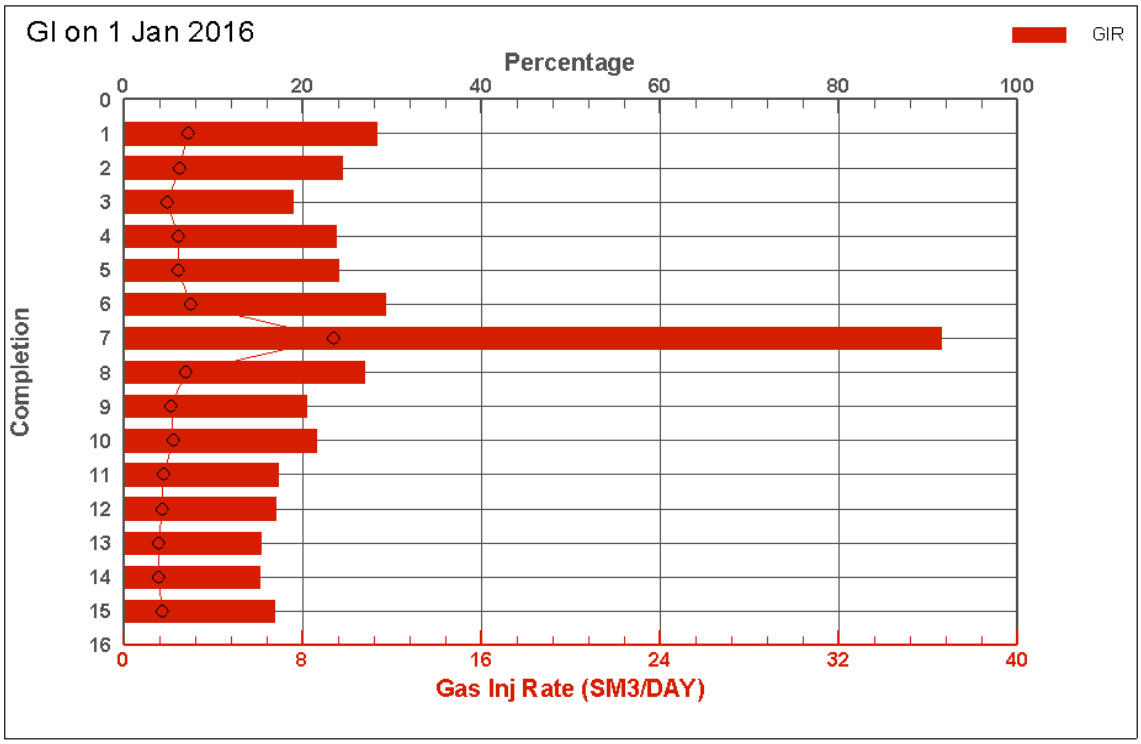

Figure 20 Gas-injection rate in the grid blocks along the perforated length of gas-injection well for the case when the sheets of grid blocks perpendicular to the injection wells are isolated from each other.

The peak in the gas injection rate in grid block 7 is an anomaly due to the influence of the production well, which is located on the opposite side in the 7th grid block. Evidently the horizontal permeability is not large enough in the sheet of grid blocks with the production well, and flow directly to the production well is favored.

3.7 Reservoir longer than the perforated length of the injection well

Jamshidnezhad et al. (2010) state that non-uniform injection correlates weakly with gas-injection pressure but much more strongly with the difference between gas- and water-injection pressures. They further speculate that effects of gas flow on hydrostatic pressure, and therefore on gas-injection pressure, may also play a role in the non-uniform injection behavior of the gas injection. Mahalle (2013) varies the position of injection wells to observe the effect of difference between the injection-well pressures. Mahalle (2013) conclude that placing the injection wells close to each other gives a more uniform injection but (based on 2D studies) may not result in good volumetric sweep. To further study the effect of well design (position, length, completion, etc.), we simulate a few scenarios in which the well is not completed throughout the width of the reservoir.

Figure 21 shows three scenarios with different well schematics and the respective gas injection rate in the grid blocks along the gas injection well at steady state. In both scenarios, 1 and 2, the water injector is completed up to the length of gas injector. In both scenarios, we see that most of the gas issues from that end of the gas injection well where the wells are not completed to the edge of the reservoir, i.e. toe of the gas injector in scenario 1 and heel in scenario 2. We believe that in those regions there is no impedance to the vertical (upward) flow of gas because of the absence of the water injector above that region, the presence of which, would have otherwise impeded the vertical flow of gas by exerting an additional hydrostatic pressure because of downward movement of injected water. To validate and substantiate the argument, we simulate scenario 3, in which the water injection well is completed along the entire length of the reservoir, but the gas injection well is completed up to some distance along the length of the reservoir. The result of scenario 3 (see **Figure 21**) shows that most of the gas issues from the heel of the gas injector, unlike scenario 1, in which the gas issues from the toe of the gas injector. The extended length of the water injector (beyond the length of the gas injector) injects water and impedes the vertical flow of gas from the underlying grid blocks. This study further supports the argument of Jamshidnezhad et al. (2010) that hydrostatic pressure may be one of the drivers of non-uniformity and instability in the gas injection.

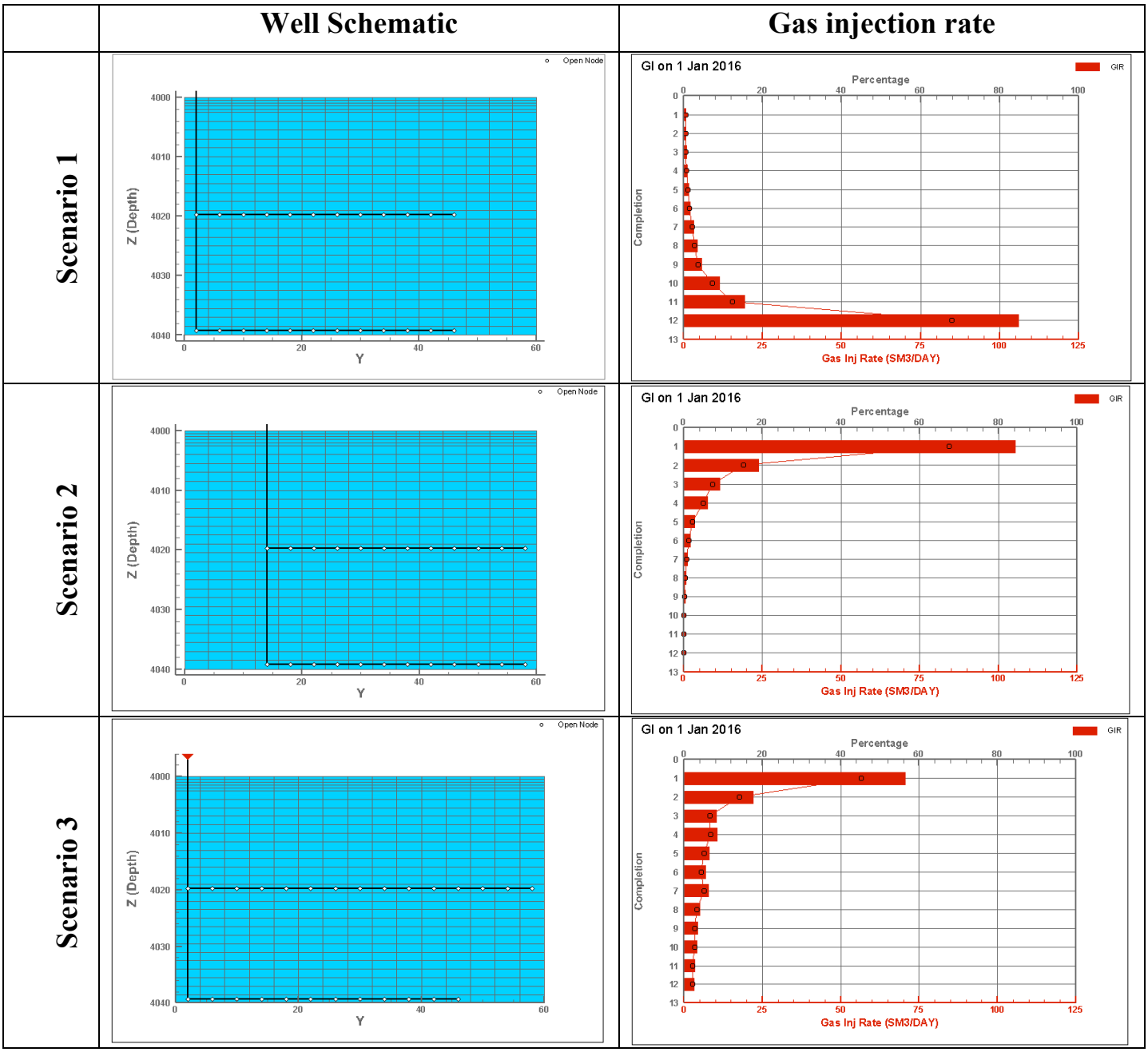

Figure 21 Left: schematic of water-injection well (upper) and gas-injection well (lower); right: plot of gas-injection rate in the grid blocks along the gas injector for various scenarios.

3.8 Effect of gas flow on hydrostatic pressure

Jamshidnezhad et al. (2010) and Mahalle (2013) suggest that instability depends on the relation between gas saturation and gas relative permeability. Their hypothesis also suggests that the effect of gas flow on hydrostatic pressure, and thus pressure difference between gas-injection well and the surrounding grid blocks, may play a role in the instability. We investigate and examine this hypothesis by studying the simulation results of the base case, i.e., pressure, saturation, relative permeability and injection rate.

Figure 22 shows the pressure in the well over the perforated length of the gas injection well in absence of frictional pressure drop. We see that the pressure in the well is uniform, which is what we expect in the absence of frictional loss. However we see a pressure gradient in the grid blocks along the gas injector. **Figure 23** shows the pressure in the grid blocks along the perforated length of the gas injection well.

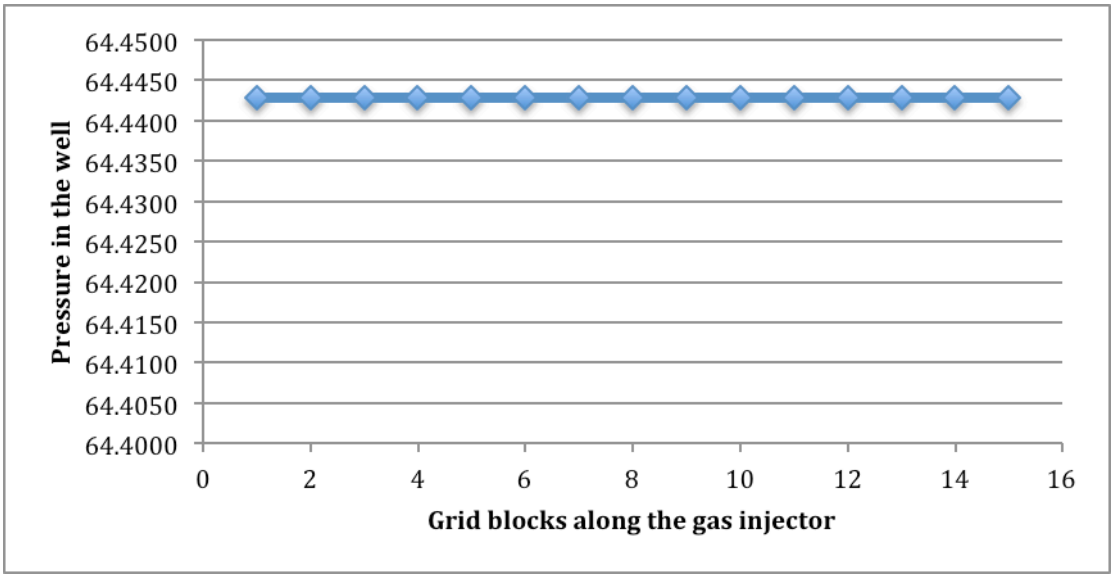

Figure 22 Pressure in the wellbore over the perforated length of the gas-injection well. (Frictional loss not included)

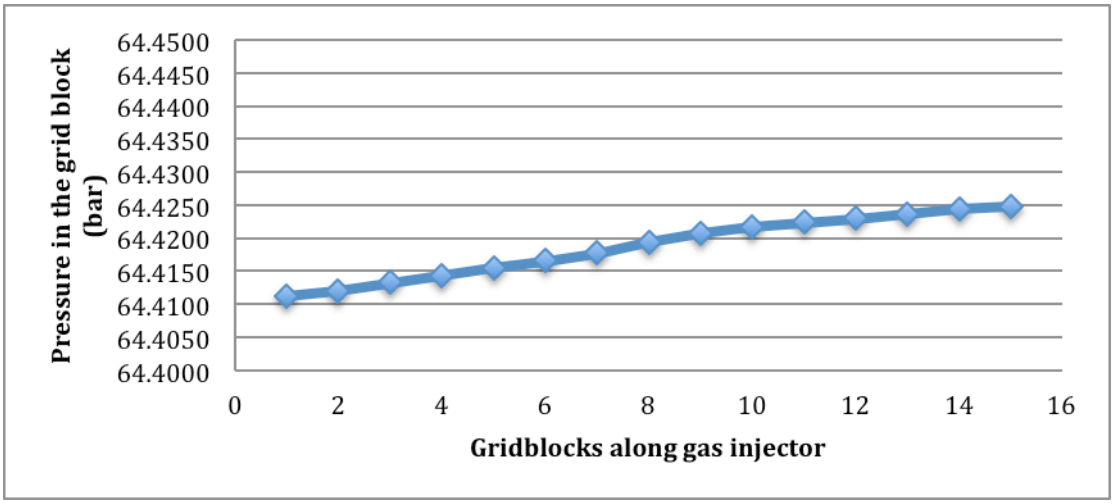

Figure 23 Pressure in the grid blocks over the perforated length of the gas-injection well. (Frictional loss not included)

The pressure in the grid blocks at the far end of the perforation (toe) is higher than the pressure at the near end of the perforation (heel). This causes the injection rate per unit length of well to fall off towards the toe of the well. We see, in **Figure 24**, higher gas saturation at the heel than the toe of the well. This increase in saturation at the heel of the well increases the relative permeability of gas in that region. **Figure 25** shows the relative permeability of gas in the grid blocks over the perforated length of the gas injection well. This increase in relative permeability at the heel reinforces the increased injection rate. **Figure 26** shows the gas-injection rate over the length of the gas-injection well.

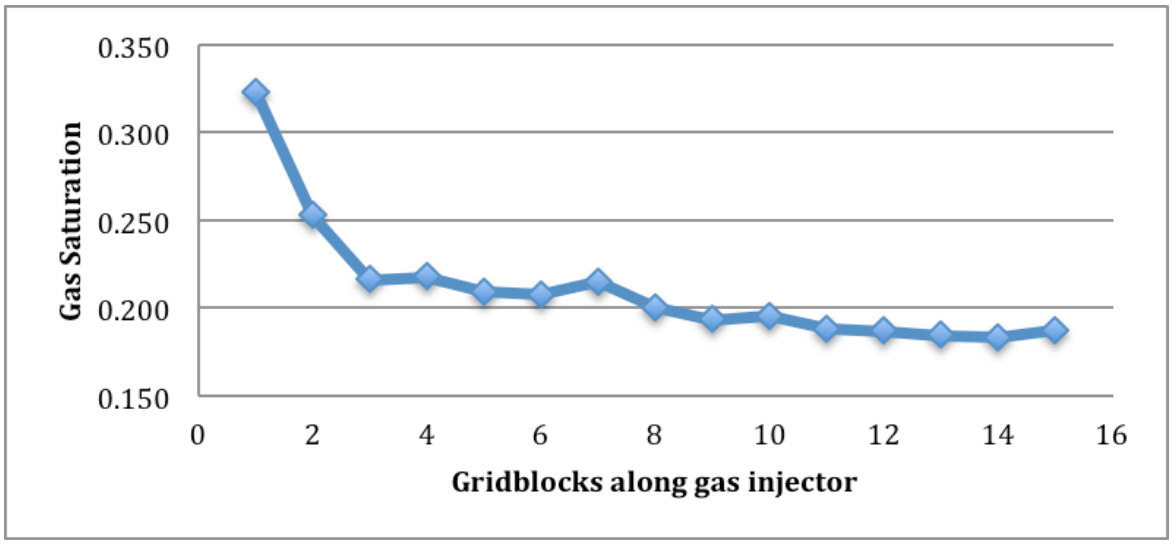

Figure 24 Saturation of gas in the grid blocks over the perforated length of the gas injection well. (Frictional loss not included)

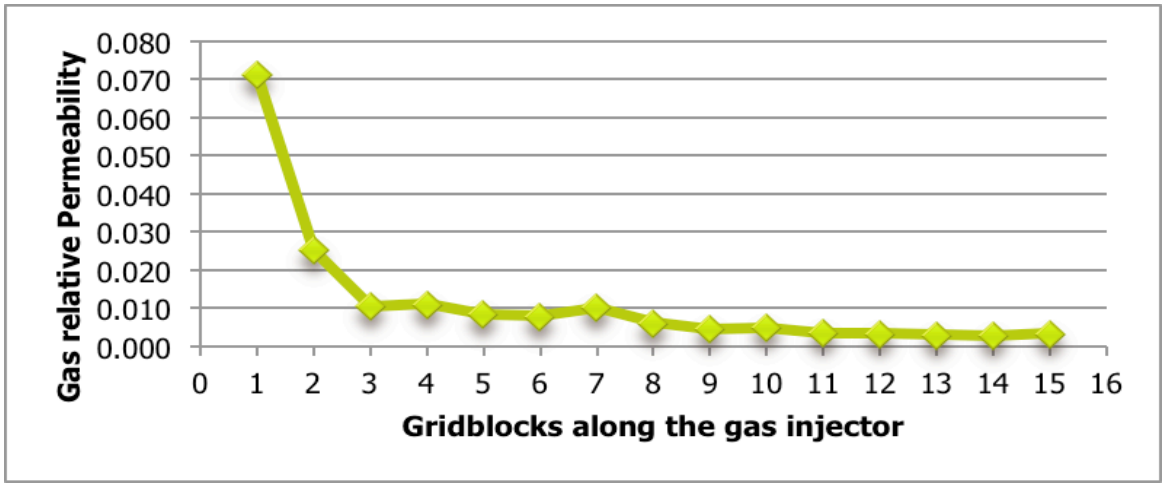

Figure 25 Relative permeability of gas in the grid blocks over the perforated length of the gas injection well. (Frictional loss not included)

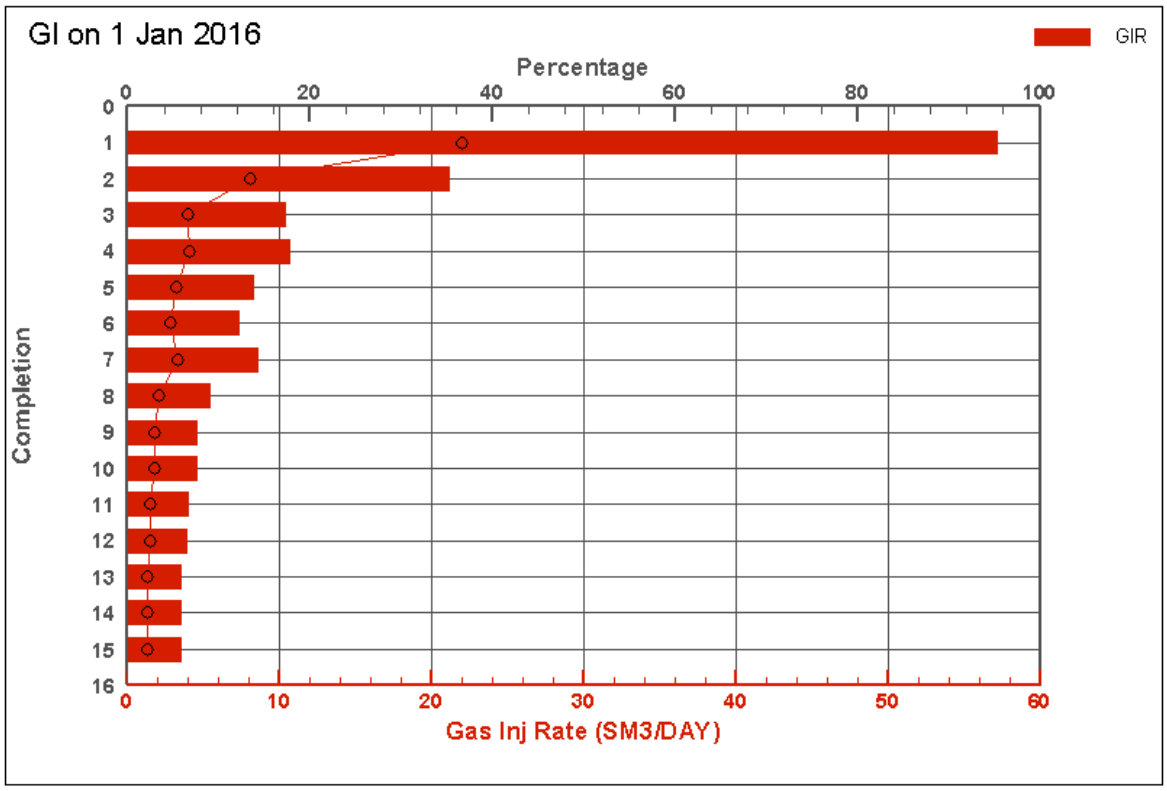

Figure 26 Gas-injection rate over the perforated length of the gas-injection well. (Frictional loss not included)

But the question arises why we see a pressure gradient in the grid blocks along the gas injector in the first place? Why is the pressure in the grid block at the toe of the well higher than the pressure at the heel even when drag along perforated length has not been accounted for?

To find out the solution, we examine the pressure in the grid blocks. We quantify the pressure due to water and gas saturations in the grid blocks overlying the grid blocks along the length of the gas-injection well. Refer **Appendix C** for the details of the method and equations used to estimate the hydrostatic pressure, accounting for both water and gas saturations.

Figure 27 shows hydrostatic pressure (accounting for both water and gas) on the grid blocks along the perforated length of the gas injection well. We see higher pressure at the far end of the perforated length than the near end. This hydrostatic pressure, exerted on the underlying grid blocks due to the water and gas column in the overlying grid blocks, puts an additional pressure in the grid blocks at the far end of the perforated length. The magnitude of our estimate in **Figure 27** is about 20 times higher than the actual pressure difference in **Figure 23**. This is because we estimated the pressure using gas density at standard condition. In ECLIPSE, we input density of gas at standard condition. The estimated hydrostatic pressure **(Figure 27)** would have been more close to the pressure in the grid blocks (**Figure 23**), if we somehow knew the density of gas at reservoir condition from the ECLIPSE. Nevertheless, the trend in estimated hydrostatic pressure is in the same direction as in the pressure in the gas-injection-well grid blocks. This may explain the reason behind the pressure gradient in **Figure 23.**

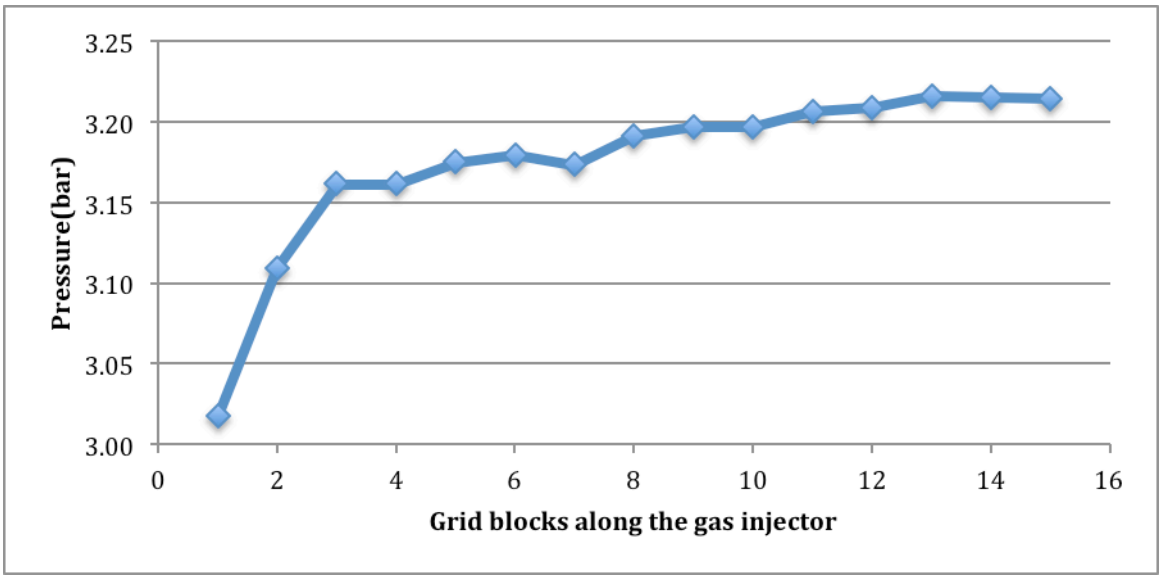

Figure 27 Hydrostatic pressure (accounting for both water and gas) on the grid blocks over the perforated length of the gas injection well.

This non-uniform distribution of hydrostatic pressure (accounting for both water and gas) increases the grid-block pressure at the far end of the perforated length. This causes the injection per unit length to fall off towards the toe of the well, which ultimately leads to higher gas saturation at the heel of the well. The increased gas saturation near the heel leads to increased gas relative permeability and further reinforces the increased injection rate at the near end of the perforated length.

3.9 Segmented Gas-Injection Well

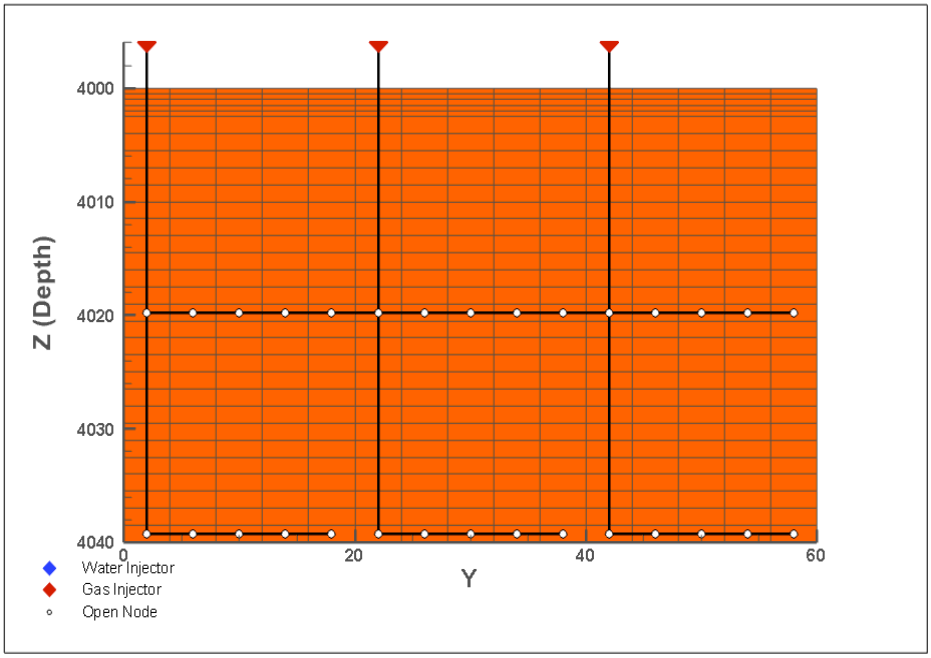

Figure 28 Schematic of reservoir model with proposed injection scheme. One water injection well (top) and three separate gas-injection wells (bottom).

A possible solution to prevent non-uniform injection behavior would be to introduce separate well segments with controlled injection rate in each segment. This segmentation would allow the gas to issue from a number of locations along the gas injection well.

We examine the proposed injection scheme (**Figure 28**) on the base case to study and compare the results with that of the base case. We keep all the other properties of the reservoir and fluid the same as those of the base case. The water injector is placed in the middle of the formation as in the base case. We introduce three separate horizontal gas-injection wells (GI1, GI2 and GI3) instead of one injection well, with the same fixed injection rate for each segment and equal segment length.

Figure 29 shows the results for this case. In the first segment (well GI1), we see that relatively most of the gas issues from grid block 1, i.e. the heel of well GI1. In the second segment (well GI2), most of the gas issues from the 7^{th} grid block, i.e. second grid block of well GI2. This is because of presence of production well in the 7^{th} grid block on the opposite face of the reservoir, which causes a preferential pathway for injected gas. We tried to remove the effect of the production well on the injection by giving a very-high permeability value in the *y*- and *x*-directions in the sheet of grid blocks containing the production well. However introduction of an extremely high permeability value causes huge pressure drop near the production well leading to shut down of the production well. We believe that if we had removed the effect of the production well, then most of the gas would come out from one end of the well or the other, i.e. heel or toe. In well segment GI3, more gas issues from the toe. Nonetheless, comparing the injection behavior of the segmented well to the base case (**Figure 4**) shows that this injection scheme makes the injection more uniform.

Segmented gas injection could be one of the methods to deal with the non-uniform nature of gas injection. The results of segmented gas injection show that a more uniform injection can be achieved through this method.

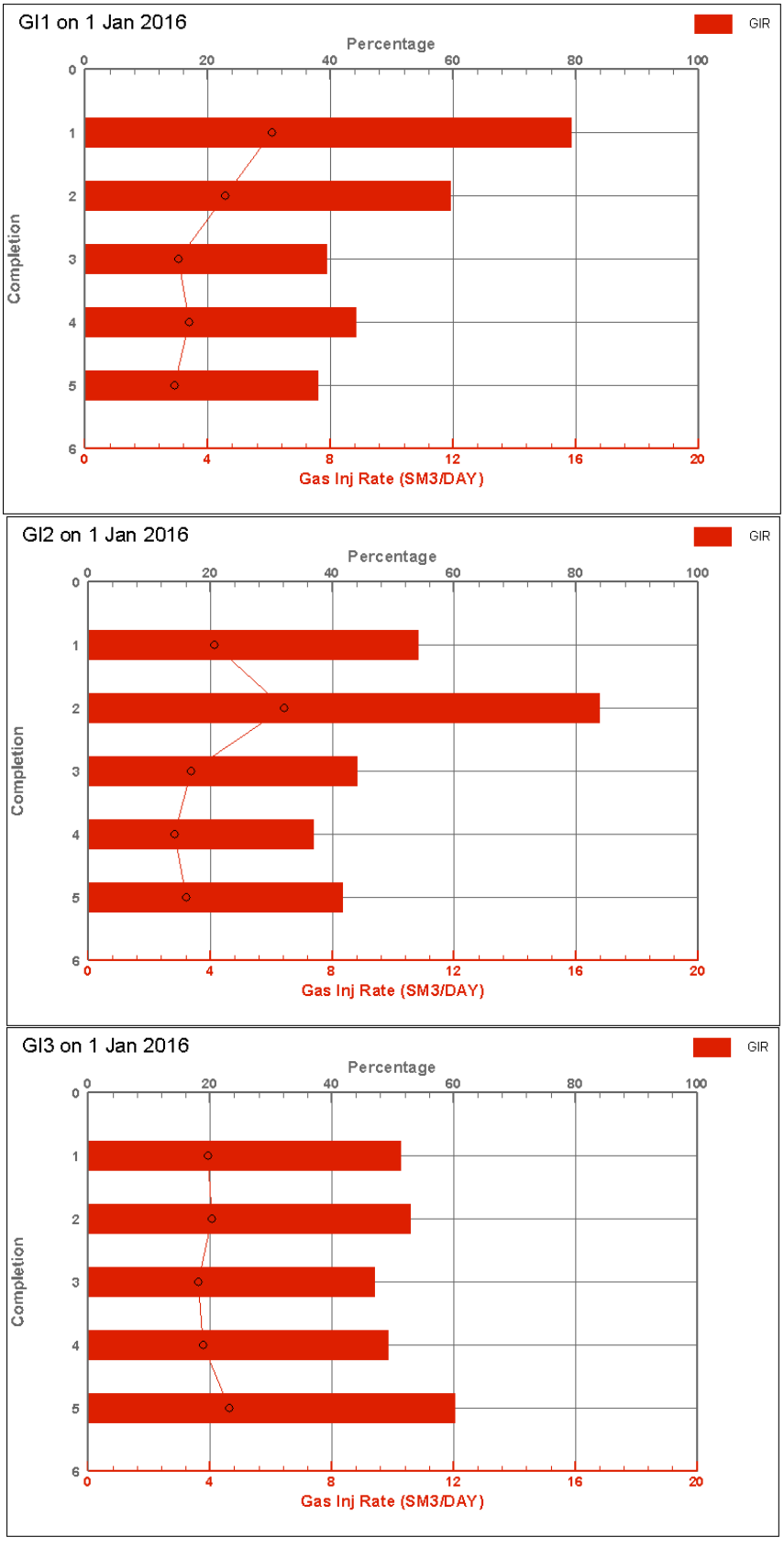

Figure 29 Gas-injection rate in the grid blocks along the gas-injection well for each segment (GI1, GI2 and GI3).

4

Discussion

Non-uniform behavior of gas injection along the perforated length of the gas-injection well seems to arise as a result of coupled effects of gas saturation, gas relative permeability, gas injectivity and the effect of gas flow on hydrostatic pressure, and subsequently on gas injection pressure. The feedback of one factor onto another may be the reason behind the instability associated with gas injection.

Grid refinement around the injection well doesn't seem to stop non-uniform injection as suggested by Mahalle (2013). Non-uniform injection behavior is not an artifact of using grid blocks that are too large for the injection well, and local grid refinement around injection well does not solve the problem. However, Mahalle's conjecture that adjacent grid blocks interact in causing non-uniform injection seems true.

Increasing non-uniformity of gas injection doesn't correlate with decreasing injection rate as suggested by Jamshidnezhad (2010). We observe that decreasing injection rate makes the injection (relatively) more uniform; however, the non-uniformity still persists.

Our analytical study of the sensitivity of injectivity to relative permeability shows that, even though an increase in gas injection rate increases the gas relative permeability significantly, the correlation between relative permeability and injectivity do not alone dictate non-uniform injection behavior.

Jamshidnezhad et al. (2010) speculates that the effect of gas flow on hydrostatic pressure may play an important role in non-uniform behavior of gas injection. We examined this speculation and found that indeed hydrostatic pressure may be involved in the non-uniform injection behavior of gas injection.

The question still remains unanswered: what initiates the instability for the first time? The non-uniform distribution of hydrostatic pressure increases the grid-block pressure at the far end of the perforated length. This causes the injection per unit length of well to fall off towards the toe of the well, which ultimately leads to high gas saturation at near end of the perforated length, i.e., heel of the well. The increased gas saturation near the heel leads to increased gas relative permeability and further reinforces the increased injection rate at the near end of the perforated length. This self-reinforcing cycle, leading to injection of more and more gas at one end of the gas-injection well, describes how the instability proceeds. But we are still not sure what initiates it in the first place. One speculation is that the effect of gas flow on hydrostatic pressure, leading to different hydrostatic pressure on to the grid blocks along the gas injection well and therefore different injection pressure, may be the point of initiation of instability. But then, why do we see different hydrostatic pressure in the first place when the reservoir is homogenous? It seems like the question of

which came first: egg or chicken? We are not sure of the initiation of the cycle leading to non-uniform injection.

ECLIPSE uses the Peaceman well-model equation. The assumption associated with the Peaceman well model is that it is derived for a vertical well. While a vertical well drains a cylindrical volume, a horizontal well drains an ellipsoid. The zone of influence is elliptical, with end points of the well constituting the foci of the ellipse (Belijn et al., 1992). This suggests that we should look out for other well models, which account for deviated and horizontal wells.

5

Conclusions

The following conclusions can be drawn from the 3D simulation study:

- Non-uniform injection is not a simulation artifact of poor gridding near the injection well. Neither grid refinement around the injection well (LGR) nor fine-grid modeling seems to be the solution to non-uniform injection along the perforated length of gas injection well.
- Increasing gas injection rate correlates with increasing non-uniformity of gas injection. Decreasing gas injection rate leads to relatively more-uniform gas-injection behavior. This result contradicts the conclusions of Jamshidnezhad et al. (2010), who suggest it is other way around, i.e., increasing non-uniformity of gas injection correlates with decreasing injection rates.
- Decreasing gas saturation exponent (n_g) in Corey's 2-phase model and decreasing gas viscosity (μ_g) leads to more-uniform injection. With smaller values of n_g and μ_g, we expect greater gas mobility. The results in both the cases suggest that increasing gas mobility leads to relatively more uniform injection.
- We examined the speculations made by Mahalle (2013) that adjacent grid blocks affect the gas injection behavior. When there is no connection between neighboring grid blocks along the gas injection well (extended in x- and z-direction), the gas injection behavior is more uniform.
- As suggested by Jamshidnezhad et al. (2010), we examined the effect of gas flow on hydrostatic pressure, and therefore on gas injection pressure. We conclude that, indeed, hydrostatic pressure is involved in the non-uniform injection behavior of the gas injection.
- A possible explanation for the instability can be that the non-uniform distribution of hydrostatic pressure increases the grid block pressure at the far end of the perforated length, which causes the injection per unit length of well to fall off towards the toe, which ultimately leads to high gas saturation near heel of the well. The increased gas saturation near the heel leads to increased gas relative permeability and further reinforces the increased injection rate at the near end of the perforated length.
- We believe that the non-uniformity in gas injection is a result of coupling of various factors, such as gas saturation, gas relative permeability, gas injectivity, the effect of gas flow on hydrostatic pressure, and effect of adjacent grid blocks. When coupled together they form the self-reinforcing cycle leading to non-uniform behavior of gas injection, with most of the gas issuing from one end of the well.
- Segmented gas injection helps ensure that gas issues from most of the perforations along the gas injection wells. This gives better sweep than the case when segmentation is not applied.

References

Algharaib, M., Gharbi, R., Malallah, A. and Al-Ghanim, W. 2007. Parametric Investigation of a Modified SWAG Injection Technique. Paper SPE 105071-MS, 15th SPE Middle East Oil & Gas Show and Conference, Kingdom of Bahrain, 11-14 March 2007. DOI: 10.2118/105071-MS

Beljin, M.S. and G. Losonsky, 1992, "HWELL, A Horizontal well Model," in Solving Ground Water Problems with Models, International Ground Water Modeling Center and the Association of Ground Water Scientists and Engineers, pp. 45-54.

Chen, H. Li, D. Yang, P. Tontiwachwuthikul, 2009. Optimal Parametric Design for Water- Alternating-Gas (WAG) Process in a CO2 Miscible Flooding Reservoir, Proceeding of Canadian International Petroleum Conference, 16 - 18 Jun.

Gharbi, R.B.C. 2003. Integrated Reservoir Simulation Studies to Optimize Recovery from a Carbonate Reservoir. Paper SPE 80437 presented at the SPE Asia Pacific Oil and Gas Conference and Exhibition, Jakarta,15–17 April. doi: 10.2118/80437-MS.

Green, D.W. and Willhite, G.P. 1998. Enhanced Oil Recovery. SPE Textbook Series, U.S.A.

Jamshidnezhad, M., Chen, C., Kool, P. and Rossen, W.R. 2008. Well Stimulation and Gravity Segregation in Gas Improved Oil Recovery. Paper SPE 112375-MS, SPE International Symposium and Exhibition on Formation Damage Control, Lafayette, Louisiana, U.S.A., 13-15 February 2008. DOI: 10.2118/112375-MS

Jamshidnezhad, M., van der Bol, L. and Rossen, W.R. 2010. Injection of Water above Gas for Improved Sweep in Gas IOR: Non-uniform Injection and Sweep in 3D. SPE Reservoir Evaluation & Engineering 13 (4): 699-709. Paper SPE 12556-PA. DOI: 10.2118/138443-PA.

Jenkins, M.K. 1984. An Analytical Model for Water/Gas Miscible Displacements. Paper SPE 12632 presented at the SPE/DOE Enhanced Oil Recovery Symposium, Tulsa, 15–18 April. doi: 10.2118/12632-MS.

Lake, L.W. 1989. *Enhanced Oil Recovery*. Englewood Cliffs, New Jersey, USA: Prentice Hall.

Ma, T.D., Rugen, J.A., Stoisits, R.F. and Youngren, G.K. 1995. Simultaneous Water and Gas Injection Pilot at the Kuparuk River Field, Reservoir Impact. Paper SPE 30726-MS, SPE Annual Technical Conference and Exhibition, Dallas, U.S.A., 22-25 October 1995. DOI: 10.2118/30726-MS.

Mahalle, N., "Injection of water above gas for improved sweep in Gas IOR: Non-uniform Injection and Sweep," MSc thesis, Dept. of Geoscience and Engineering, TU Delft, 2013

Peaceman, D.W. 1978. Interpretation of Well-Block Pressures in Numerical Reservoir Simulation, SPE J. 18(3): 183-194; Trans., AIME, 265. SPE 6893-PA. DOI:10.2118/6893-PA.

Quale, E.A., Crapez, B., Stensen, J.A. and Berge, L.I. 2000. SWAG Injection on the Siri Field – An Optimized Injection System for Less Cost. Paper SPE 65165-MS, SPE European Petroleum Conference, Paris, France, 24-25 October 2000. DOI:10.2118/65165-MS.

Rossen, W.R. and Shen, C. 2007. Gravity Segregation in Gas-Injection IOR. Paper SPE 107262-MS, EUROPEC/EAGE Conference and Exhibition, London, 11-14 June 2007. DOI: 10.2118/107262.

Rossen, W.R., van Duijn, C.J., Nguyen, Q.P. and Vikingstad, A.K. 2010. Injection Strategies to Overcome Gravity Segregation in Simultaneous Gas and Liquid Injection into Homogeneous Reservoirs. SPE J. 15 (1): 76-90. SPE 99794-PA. DOI: 10.2118/99794-PA

Schlumberger, Geoquest: ECLIPSE Reference Manual and Technical Description, version 2013.1.0.0.

Stone, H.L. 1982. Vertical Conformance in an Alternating Water-Miscible Gas Flood. Paper SPE 11130-MS, SPE Annual Technical Conference and Exhibition, New Orleans, U.S.A., 26-29 September 1982. DOI: 10.2118/11130-MS.

Stone, H.L. 2004. A Simultaneous Water and Gas Flood Design with Extraordinary Vertical Sweep. Paper SPE 91724. Paper SPE 91724-MS, International Petroleum Conference, Puebla Pue., Mexico, 7-9 November 2004. DOI: 10.2118/91724-MS.

van der Bol, L. 2007. Evaluation in Three Dimensions of Injection of Water above Gas for Improved Sweep in Gas IOR. MSc thesis, Delft University of Technology, Delft, The Netherlands, August 2007.

Waggoner, J.R., Castillo, J.L. and Lake, L.W.: 'Simulation of EOR Processes in Stochastically Generated Permeable Media,' SPE 21237, SPE Formation Evaluation, 173-180, June 1992.

Zekri, A. Y., Nasr, M. S., & AlShobakyh, A. (2011, January 1). Evaluation of Oil Recovery by Water Alternating Gas (WAG) Injection - Oil-Wet & Water-Wet Systems. Society of Petroleum Engineers. doi:10.2118/143438-MS

Appendix

A

Appendix-A: Reservoir and Fluid parameters

Relative-Permeability Functions

We use relative-permeability function as described in the work of Mahalle (2013).

$$k_{ro} = 0$$

$$k_{rg} = k_{rg}^{*}\left[\frac{\left(S_g - S_{gc}\right)}{\left(1 - S_{wc} - S_{gc}\right)}\right]^{n_g}$$

$$k_{rw} = k_{rw}^{*}\left[\frac{\left(S_w - S_{wc}\right)}{\left(1 - S_{wc} - S_{gc}\right)}\right]^{n_w}$$

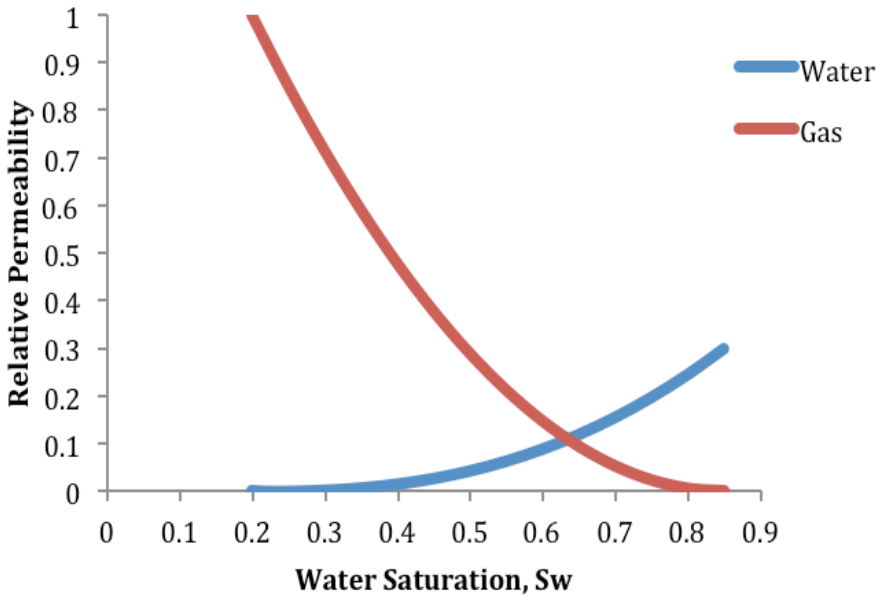

Figure 30 Relative-permeability function and curve as applied in the work of Mahalle (2013)

The end-point values and saturation exponents are constant in all the simulated cases unless mentioned otherwise.

Table 1 End-point values and saturation exponents

k_{rw}^{*}	**0.3**
k_{rg}^{*}	**1**
S_{wc}	**0.2**
S_{gc}	**0.15**
S_{or}	**0**
n_g	**2**
n_w	**2.5**

Table 2 Overview of reservoir and fluid parameters used in the simulator

Reservoir parameters		
Horizontal permeability (in *x*- and *y*-direction)	1000*	mD
Vertical permeability (in *z*-direction)	210*	mD
Porosity	0.25	-
Fluid parameters		
Gas		
Density, at surface conditions	1.09	Kg/m^3
Viscosity at reservoir condition	0.0144	cP
Water		
Density, at surface condition	1000	Kg/m^3
Viscosity at surface condition	1	cP
* If mentioned otherwise		

Compressibility

Water is incompressible. However, ECLIPSE doesn't accept zero compressibility for gas. Therefore we make the gas almost incompressible by varying gas formation volume factor (B_g) in such a way that the B_g value doesn't change much with increasing pressure. For instance, from 140 to 159 bar gas volume shrinks by only 0.16%.

Table 3 Gas formation volume factor at respective pressures.

Pressure (Bar)	Bg
1.0	0.132250
10.0	0.132248
24.9	0.132222
39.8	0.132109
54.7	0.131948
69.6	0.131408
84.5	0.130978
99.4	0.130385
114.3	0.129800
129.2	0.129400
140.0	0.129000
159.0	0.128800
173.9	0.128500
188.8	0.128000
203.7	0.127700
218.6	0.127600
233.5	0.127400
248.4	0.127280
263.3	0.127000
278.2	0.126800
293.1	0.126570
308.0	0.126290
322.9	0.126000
350.0	0.125600
400.0	0.124200
450.0	0.123500
500.0	0.122800

Appendix

B

Appendix B: Sensitivity study of injection rate on relative permeability

We do an analytical study to examine the effect of injection rate on relative permeability and check whether they are solely responsible for the non-uniform behavior of the gas injection or not. We hope to see how a percentage change in injection rate affects the relative permeability of gas and hence the gas mobility. We carry out the study on our base case model.

We have gas saturation (S_g) and gas injection rate (q_g) in each grid block along the perforated length of gas injection well from the simulation results.

$$f_g = \frac{\frac{k_{rg}}{\mu_g}}{\frac{k_{rg}}{\mu_g} + \frac{k_{rw}}{\mu_w}} \quad \text{.....(B1)}$$

$$f_g = \frac{q_g}{q_g + q_w} \quad \text{.....(B2)}$$

Using the relation between relative permeability and saturation as listed in **Appendix A** and **Equation B1** and **B2**, we calculate fraction of gas (f_g) and hence water flux (q_w) in each grid block along the gas injection well. Now we fix the q_w and slightly increase the gas injection rate and back-calculate the gas fraction (f_g) and subsequently calculate the relative permeability of gas and gas saturation. We simulate three cases each at different stages of gas injection, i.e., at the time of initiation of instability (around 16th Jan 2015) and at steady state (at the end of 1 year). In first case, we increase the gas injection rate by 2% of the base case; in second case, we increase the gas injection rate twice the value of the base case; and in third case, we make the injection rate 10 times that of the base case. The results of which are shown in **Figure 31**.

The results show that an increase in injection rate increases the gas saturation and gas relative permeability quite significantly. In the first case, at the time of initiation of instability, when we increase the gas injection rate by 2%, we see a 0.3% increase in gas saturation and 1.7% increase in gas relative permeability. However, in case 3, when the injection rate is increased by 900% (10 times the injection rate of the base case), we see that gas saturation increases by 50%, but the relative permeability increases by almost 450%. Similarly, we can study the result at steady state (at the end of one year).

Initial time step 16th Jan 2015

	Qgas (kg/m3)			Sgas			Krg		
	Case 1	Case 2	Case 3	Case 1	Case 2	Case 3	Case 1	Case 2	Case 3
Old	15.8387232	15.8387232	15.8387232	0.240	0.240	0.240	0.019095	0.019095	0.019095
New	16.1554976	31.6774464	158.387232	0.241	0.269	0.360	0.019412	0.033433	0.104397
%change	2	100	900	0.3	12.1	50.1	1.7	75.1	446.7

Final time step 1st Jan 2016

	Qgas (kg/m3)			Sgas			Krg		
	Case 1	Case 2	Case 3	Case 1	Case 2	Case 3	Case 1	Case 2	Case 3
Old	57.2079582	57.2079582	57.2079582	0.323	0.323	0.323	0.071214	0.071214	0.071214
New	58.3521174	114.415916	572.079582	0.325	0.367	0.481	0.072188	0.111843	0.260085
%change	2	100	900	0.4	13.6	48.9	1.4	57.1	265.2

Figure 31 Results of sensitivity study of injection rate on relative permeability

At both injection stages, we observe that an increase in gas injection rate affects the gas relative permeability significantly. One of the speculations of Jamshidnezhad et al. (2010) on non-uniform injection behavior of gas injection is that higher gas-injection rate gives higher gas saturation near the well, which in turn increases gas relative permeability and reinforces the increased injection rate. If our study would have shown, for example, a 2% increase in injection rate causes more than 2% increase in gas relative permeability, then we might say that the instability could be explained solely by the correlation between relative permeability and injectivity. However, in our result, we see a 2% increase in gas injection rate leads to mere 1.7% or 1.4% increase in gas relative permeability. It shows that, even though an increase in gas injection rate increases the gas relative permeability significantly, it is not big enough to say that it is the relation between relative permeability and injection rate alone that dictates or initiates the non-uniform injection behavior.

Appendix

C

Appendix C: Hydrostatic pressure estimation

Jamshidnezhad et al. (2010) suggests that effect of gas flow on hydrostatic pressure, and therefore on gas-injection pressure, may play a role in the non-uniform injection behavior of the gas injection. To study the effect of effect of gas flow on hydrostatics pressure, we estimate the hydrostatic pressure on the grid blocks along the perforated length of the gas injection well.

We know gas saturation (S_g) and water saturation (S_w) in each grid block from the simulation results of the base case. We can calculate the pressure (P) due to fluids (water and gas) on each grid block along the length of the gas injection well using **Equation C1**.

$$P_{(1,j,k_{well})} = \sum_{k=1}^{k_{well}-1} [(S_g)_{(1,j,k)}\rho_g + (S_w)_{(1,j,k)}\rho_w] g h_{(1,j,k)} \quad \text{..... (C1)}$$

where, j=1(heel), 2, 3,……..n_y (toe)
ρ_g is the density of gas; ρ_w is the density of water; g is acceleration due to gravity; h is the height of each grid block (in *z*-direction), k_{well} is the location of the well in *z* –direction and n_y is the y-coordinate of the toe of the well.

Hypothetical example:

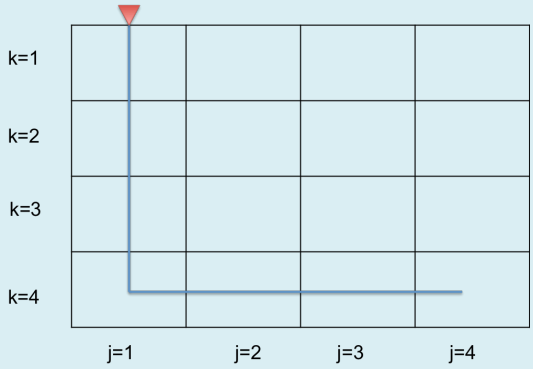

Figure 32 2D well-schematic showing a gas injection well, at coordinates (1,j,4).

If we calculate the hydrostatic pressure on a grid block along the well, e.g. the grid block at coordinate (1,1,4), then we first calculate the {(S_g*ρ_g+ S_w*ρ_w)*g*h} for each grid block in the first column (j=1; k=1, 2 and 3). The summation of {(S_g*ρ_g+ S_w*ρ_w)*g*h} of each grid block will give the hydrostatic pressure on that particular grid block along the injection well, i.e., the grid block at coordinate (1, 1, 4).

The calculated pressure is the pressure on to the grid blocks along perforated length of the gas injection well due to water and gas saturation. Each grid block has varying gas and water saturation and therefore it results in different hydrostatic pressure in the grid blocks. **Equation C1** is a hypothesized equation to calculate pressure accounting for fluid saturation. It may not be a completely accurate way to calculate the hydrostatic pressure, but it will at least give us a rough estimate of the pressure distribution. **Figure 34** shows the hydrostatic pressure distribution along the length of the gas injection well. We see higher hydrostatic pressure at the toe of the gas injection well than at the heel. However, we see that hydrostatic pressure is almost same through out the perforated length of the water injection well (see **Figure 33**).

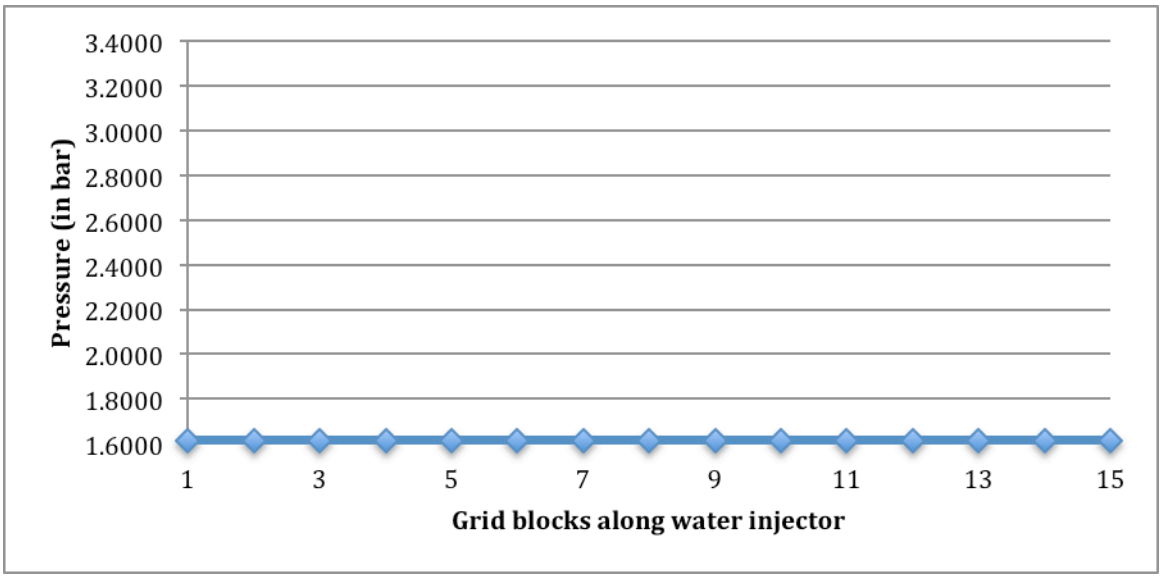

Figure 33 Hydrostatic pressures on to the grid blocks along the perforated length of water-injection well

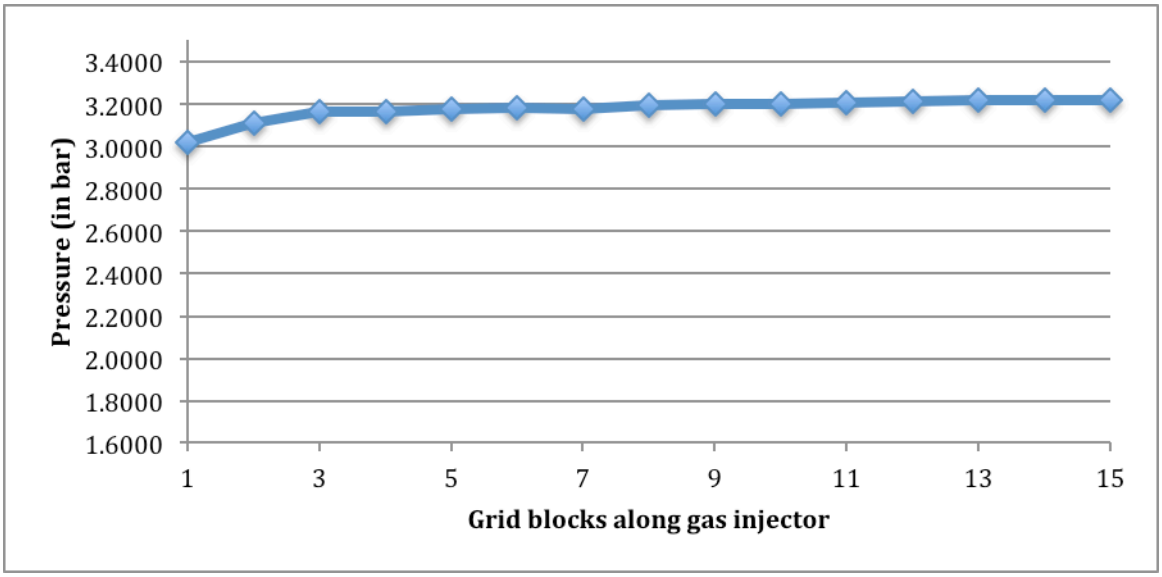

Figure 34 Hydrostatic pressures on to the grid blocks along the perforated length of water-injection well

Appendix

D

Appendix D: Miscellaneous

Case 1: One horizontal gas injector and one vertical production well (no water injector)

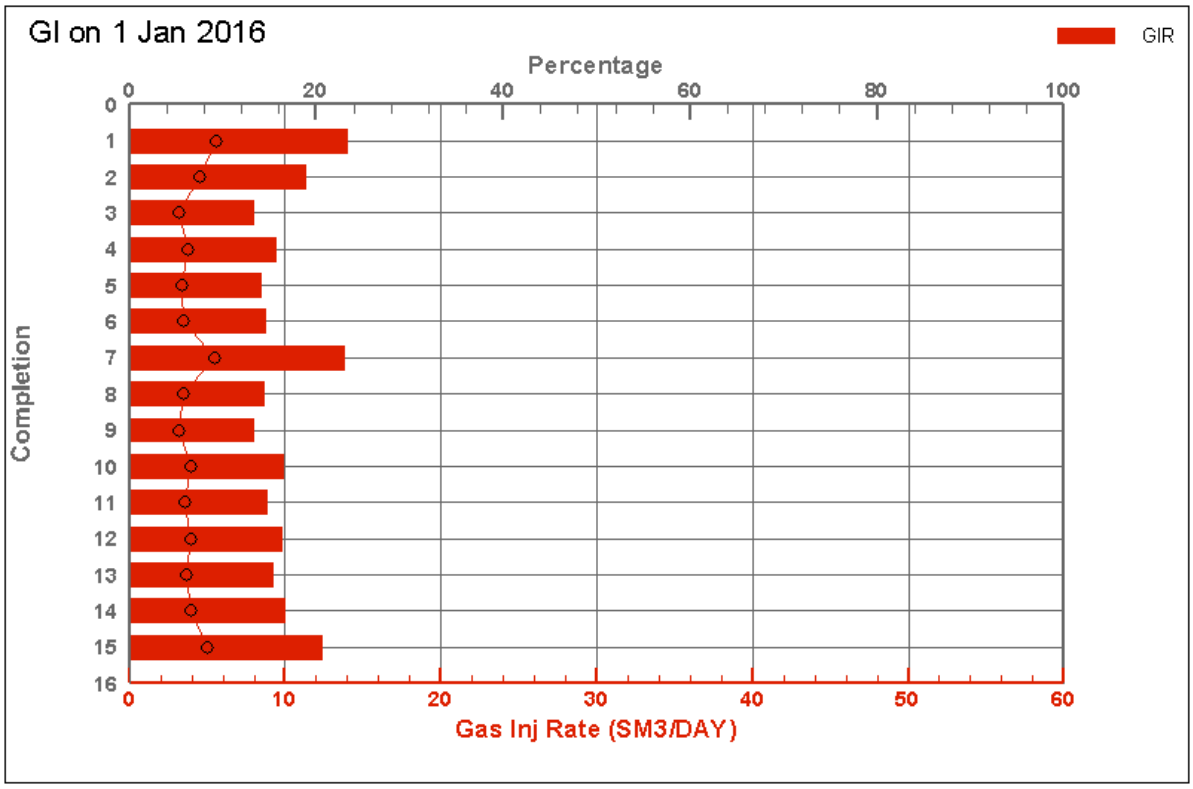

Figure 35 Gas-injection rate over the perforated length of the gas-injection well. (Frictional loss not included)

In this case, when the water injector is absent, the gas injection rate is more uniform than that of the base-case. In our base case, when the water injector is present, the injection is non-uniform. This gives us an understanding that presence of the water-injection well affects the gas-injection behavior.

Case 2: Refining grids along y-axis

Number of grid blocks in *x*-, *y*-, and *z*-direction: 32x60x30;

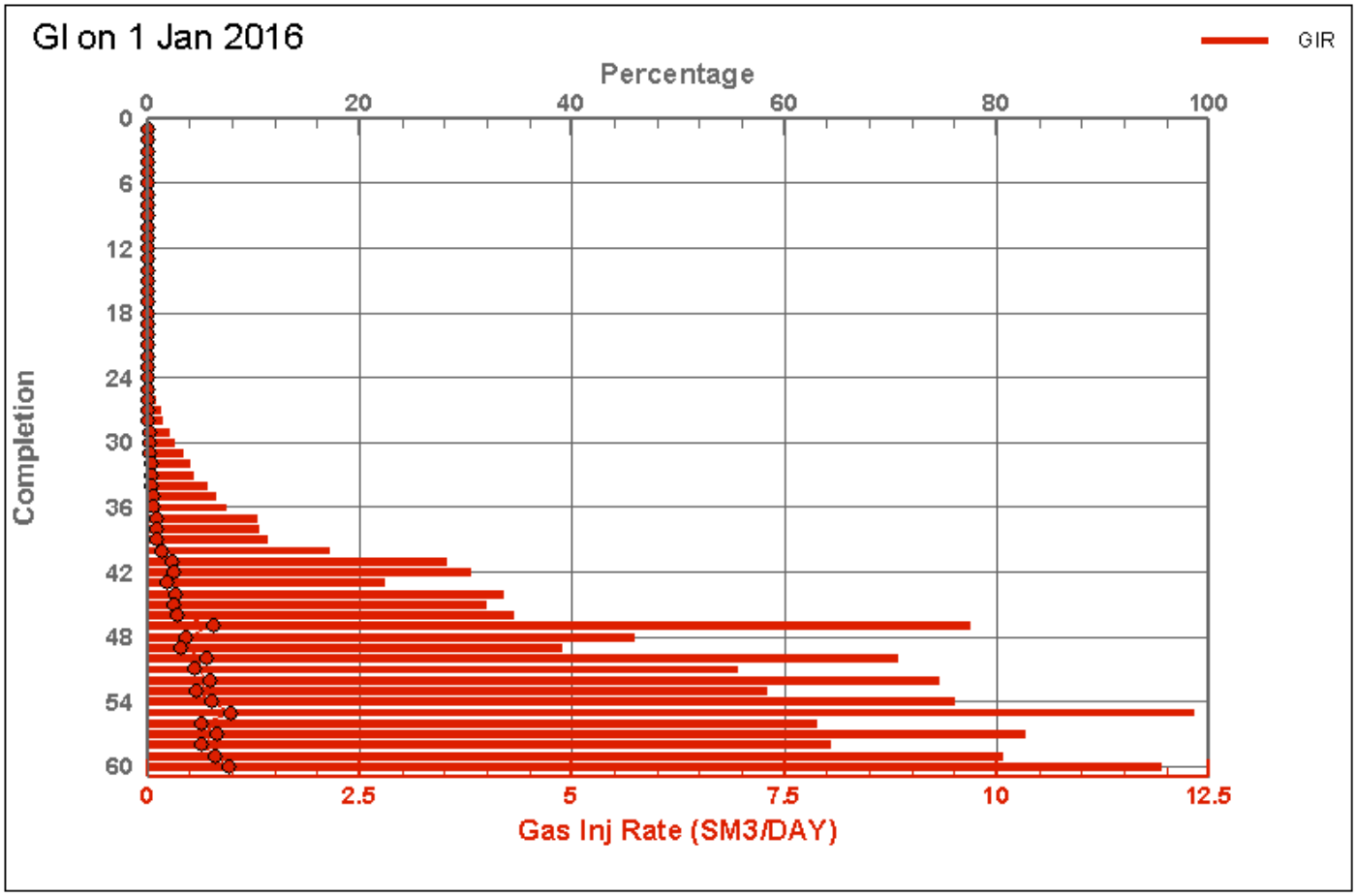

Figure 36 Gas-injection rate over the perforated length of the gas-injection well for the case of grid refinement along the *y*-axis. (Frictional loss not included)

Figure 36 shows the gas injection rate in the grid blocks along the gas injection well. We see that gas issues from the toe of the well whereas in the base-case model gas issues from the heel of the well.